Non-toxic Stx derivatives from Escherichia coli posses adjuvant activity for mucosal immunity. Vaccine 22: 3751-3761

41) Nochi, T., Yuki, Y., Terahara, K., Hino, A., Kunisawa, J., Kweon, M-N., Yamaguchi, T., and **Kiyono, H.** 2004. Biological role of Ep-CAM in the physical interaction between epithelial cells and lymphocytes in intestinal epithelium. Clin. Immunol. 113: 326-339

42) Mizushima, T., Ito, T., Kishi, D., Kai, Y., Tamagawa, H., Nezu, R., **Kiyono, H.**, and Matsuda, H. 2004. Therapeutic effects of a new lymphocyte homing reagent FTY720 in interleukin-10 gene-deficient mice with colitis. Inflamm. Bowel Dis. 10:182-192.

43) Ueta, M., Nochi, T., Jang, M-H., Park, E-J., Igarashi, O., Hino, A., Kawasaki, S., Shikina, T., Hiroi, T., Kinoshita S., and **Kiyono, H.** 2004. Intracellularly expressed TLR2s and TLR4s contribution to an immunosilent environment at the ocular mucosal epithelium. J. Immunol. 173: 3337-3347

44) **Kiyono, H.**, and Fukuyama, S. 2004. NALT-versus Peyer's-patch-mediated mucosal immunity. 2004. Nature Rev. Immunol. 4: 699-710

45) Yoshino, N., Lu, X-S. F., Fujihashi, K., Hagiwara, Y., Kataoka, K., Lu, D., Hirst, L., Honda, M., F.W. van Ginkel., Takeda, Y., Miller, C.J., **Kiyono, H.**, and McGhee, J.R. 2004. A novel adjuvant for mucosal immunity to HIV-1 gp120 in nonhuman primates. J. Immunol. 173: 6850-6857

46) Kubo-Akashi, C., IsekiI, M., Kweon, S-M., Takizawa, H., **Takatsu, K.**, and S. Takaki, S. Roles of conserved family of adaptor proteins, Lank, SH2-B and APS for mast cell development growth and functions: APS-deficiency causes impaired degranulation. 2004. Biochem. Biophys. Res. Commun. 315:356-362

47) Iseki, M., Kubo, C., Kwon, S-M., Yamaguchi, A., Kataoka, Y., Yoshida, M., **Takatsu, K.**, and Takaki, S. 2004. Negative regulatory role of APS, adaptor molecule containing PH and SH2 domains in B-1 cells and B cell receptor-mediated proliferation. Mol. Cell. Biol. 24:2243-2250

48) Tamura, T., Ariga, H., Kinashi, T., Uehara, S., Kikuchi, T., Nakada, M., Tokunaga, T., Xu, W., Kariyone, A., Saito, T., Kitamura, T., Maxwell, G., Takaki, S., and **Takatsu, K.** 2004. The role of antigenic peptide in CD4+ T helper phenotype development in a T cell receptor transgenic model. Int. model. Int. Immunol. 6:1691-1699

49) Moon, B-Y., Takaki, S., Miyake, K., and **Takatsu, K.** 2004. The role of IL-5 for mature B-1 cells in homeostatic proliferation, cell survival, and Ig production. J. Immunol. 172:6020-6029

50) Hirano, M., Y. Kikuchi, A. S. Nisitani, A. Yamaguchi, A. Sato, T. Ito, H. Iba,

and K. Takatsu. 2004. Btk enhances transcriptional co-activation activity of BAM11, a Btk associated molecule of a SWI/SNF complexes. Int. Immunol. 16: 747-57

51) Tanaka, H., M. Komai, K. Nagao, M. Ishizaki, D. KajiwaraG. and Takatsu, K. 2004. Delespesse, and H. Nagai. Role of IL-5 and eosinophils in allergen-induced airway remodeling in mice. Am. J. Resp. Cell. Mol. Biol. 31: 62-8,

52) Moon, B-M., S. Takaki, H. Nishizumi, T. Yamamoto, and Takatsu, K. 2004. Abrogation of autoimmune disease in Lyn-deficient mice by the deletion of ILL-5 receptor a chain gene. Cell. Immune. 228:110-118

53) Wen, X., D. Zhang, Y. Kikuchi, Y. Jiang, K. Nakamura, H Tsurui, K. Takahashi, M. Abe, M. Ohtsuji, H. Nishimura, K. Takatsu, T. Shire, and S. Hirose. 2004. Transgene-mediated over-expression of IL-5 inhibits autoimmune disease, but increases the risk of B-cell chronic lymphocytic leukemia in a model of murine lupus. Eur. J. Immunol. 34:2740-2749

54) Tamura. T., H. Ariga, T. Kinashi, S Uehara, T Kikuchi, M. Nakada T Tokunaga, Wen Xu, A. Kariyone, T. Saito, T. Kitamura, Gavin MaxWell, S. Takaki, and Takatsu, K.. 2004. The role of antigenic peptide in CD4+ T helper phenotype development in a T cell receptor transgenic model. Int. Immunol. 15: 1691-1699, (Featured article)

55) Inoue, H., R. Kato, S. Fukuyama, A. Nonami, K. Taniguchi, K. Matsumoto, T. Nakano, M. Tsuda M. Matsumura, M. kubo, F. ishikawa, K. Takatsu, Y. Nakanishi, and A Yoshimura. 2005. Spred-1 negatively regulates allergen-induced airway eosinophilia and hyperresponsiveness. J. Exp Med. 201: 73-82, 2005.

56) Kweon, M. N., Yamamoto, M., Rennert, P. D., Park, E. J., Lee, A. Y., Chang, S. N., Hiroi, T., Nannno, M. and Kiyono, H. 2005. Prenetal blockage of lymphotoxin beta receptor and TNF reeceptor p55 signaling cascade resulted in the acceleration of tissue genesis for isolated lymphoid follicles in large
intestine. (in press)

研究成果の刊行物・別刷り

Immunity

Volume 17 Number 1 July 2002

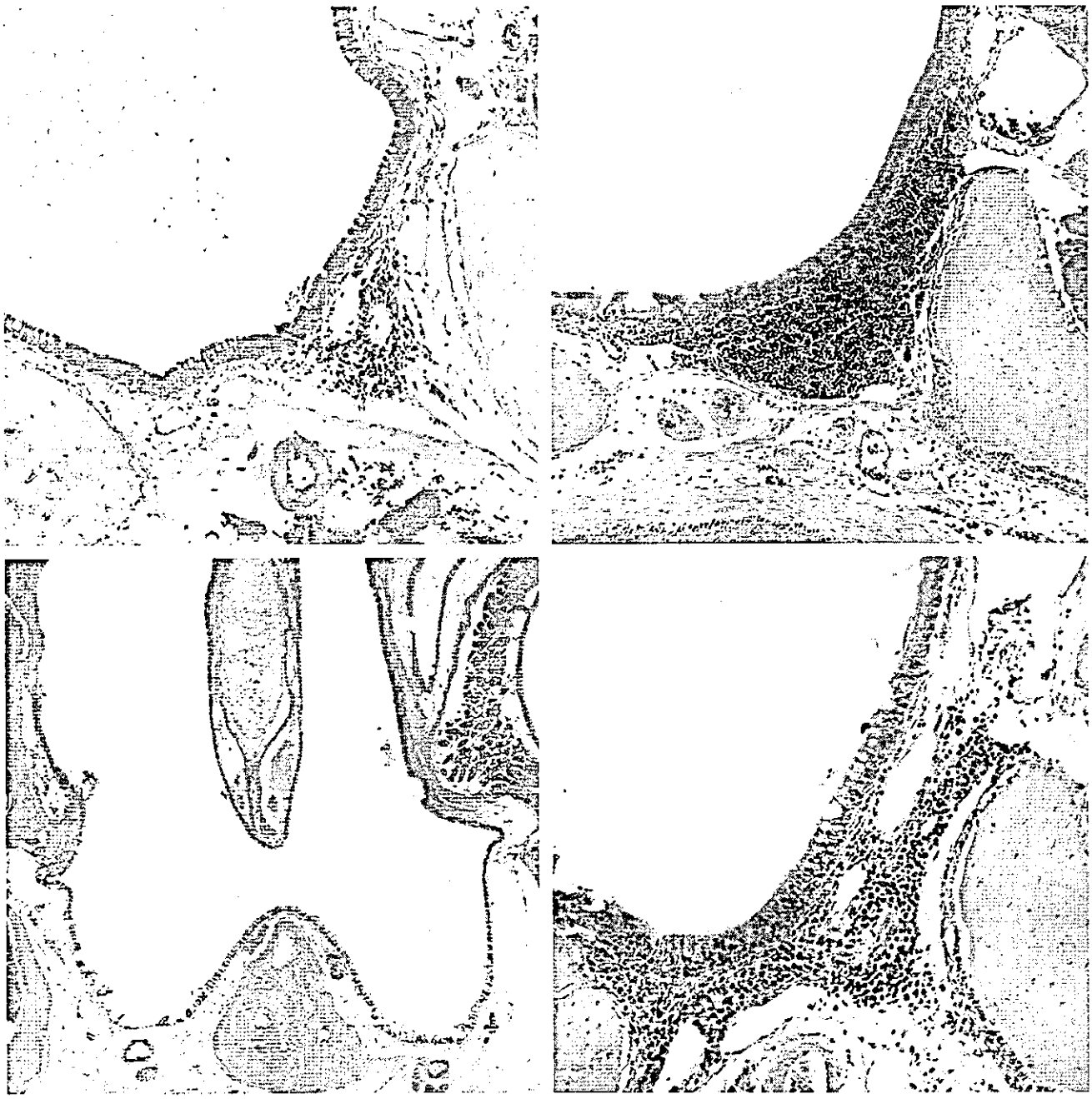

Initiation of NALT Organogenesis in Id2$^{-/-}$ Mouse

Immunity, Vol. 17, 31–40, July, 2002, Copyright ©2002 by Cell Press

Initiation of NALT Organogenesis Is Independent of the IL-7R, LTβR, and NIK Signaling Pathways but Requires the Id2 Gene and CD3⁻CD4⁺CD45⁺ Cells

Satoshi Fukuyama,[1,5] Takachika Hiroi,[1] Yoshifumi Yokota,[2] Paul D. Rennert,[3] Manabu Yanagita,[1] Naotoshi Kinoshita,[1] Seigo Terawaki,[1] Takashi Shikina,[1] Masafumi Yamamoto,[1,4] Yuichi Kurono,[5] and Hiroshi Kiyono[1,6,7,8]

[1]Department of Mucosal Immunology
Research Institute for Microbial Diseases
Osaka University
Suita, Osaka, 565-0871
[2]First Department of Biochemistry
Fukui Medical University
Matsuoka, Fukui, 910-1193
Japan
[3]Biogen Incorporated
Cambridge, Massachusetts 02142
[4]Department of Oral Medicine
School of Dentistry at Matsudo
Nihon University
Matsudo, Chiba, 271 8587
[5]Department of Otolaryngology
Faculty of Medicine
Kagoshima University
Kagoshima, 890-8520
Japan
[6]Immunobiology Vaccine Center
The University of Alabama at Birmingham
Birmingham, Alabama 35294
[7]Division of Mucosal Immunology
Department of Microbiology and Immunology
The Institute of Medical Science
The University of Tokyo
Tokyo, 108-8639
Japan

Summary

Initiation of nasopharyngeal-associated lymphoid tissue (NALT) development is independent of the programmed cytokine cascade necessary for the formation of Peyer's patches (PP) and peripheral lymph nodes (PLN), a cytokine cascade which consists of IL-7R, LTα1β2/LTβR, and NIK. However, the subsequent organization of NALT seems to be controlled by these cytokine signaling cascades since the maturation of NALT structure is generally incomplete in those cytokine cascade-deficient mice. NALT as well as PP and PLN are completely absent in Id2$^{-/-}$ mice. NALT organogenesis is initiated following the adoptive transfer of CD3⁻CD4⁺CD45⁺ cells into Id2$^{-/-}$ mice, constituting direct evidence that CD3⁻CD4⁺CD45⁺ inducer cells can provide an IL-7R-, LTα1β2/LTβR-, and NIK-independent tissue organogenesis pathway for secondary lymphoid tissue development.

[8]Correspondence: kiyono@biken.osaka-u.ac.jp

Introduction

In rodents, nasopharyngeal-associated lymphoid tissue (NALT) is an organized lymphoid structure found on both sides of the nasopharyngeal duct dorsal to the cartilaginous soft palate and is considered analogous to the Waldeyer's ring in humans (Kuper et al., 1990, 1992). NALT consists of follicle-associated epithelium (FAE), high endothelial venules (HEV) and T cell- and B cell-enriched areas. Numerous M cells, specialized for antigen sampling, are present in NALT and Peyer's patches (PP) FAE (Jeong et al., 2000). The structural similarity of NALT and PP suggests that NALT is an important inductive site for mucosal immunity in the upper respiratory tract, much like PP in the intestinal immune system. NALT has been shown to be an important site for the generation of high-affinity memory B cells (Shimoda et al., 2001). Nasal immunization with antigen (Ag) and cholera toxin (CT) as a mucosal adjuvant induces Ag-specific Th2-type responses for the generation of Ag-specific IgA-producing cells in the nasal passages and distal mucosal sites, including the genitourinary and intestinal tracts (Imaoka et al., 1998; Kurono et al., 1999; Yanagita et al., 1999). In spite of accumulated evidence demonstrating the unique structure and the importance of NALT in the mucosal immune system, little is known concerning the cellular and molecular mechanisms that control NALT development.

Lymphotoxin (LT) is a critical signaling molecule for secondary lymphoid tissue organogenesis. Lymph nodes (LN) and PP are absent in LTα-deficient (LTα$^{-/-}$) mice (De Togni et al., 1994). LTα forms LTα1β2 heterotrimers that can transduce an activation signal through the LTβ receptor (LTβR) to organize secondary lymphoid tissues (Crowe et al., 1994; Rennert et al., 1996, 1998). Our finding that the LTα1β2 heterotrimer could be antagonized by an LTβR-immunoglobulin (LTβR-Ig) fusion protein demonstrated that the timing of secondary lymphoid tissue development was regulated during embryogenesis. When LTβR-Ig was administered to pregnant mice at embryonic day 18 (E18), the offspring lacked PP but had unaltered LN formation. If the fusion protein was delivered from E12 and thereafter, PP as well as popliteal, axillary, and inguinal LN were absent, with only mesenteric LN and cervical LN retained (Rennert et al., 1997; Yamamoto et al., 2000). In IL-7 receptor α chain-deficient (IL-7Rα$^{-/-}$) mice, only the formation of PP was impaired (Adachi et al., 1998). Blocking of IL-7Rα function by a single injection of the antagonistic mAb on E15.5 resulted in PP-deficient offspring with unaltered LN (Yoshida et al., 1999). These findings indicate that well-programmed cytokine-mediated PP and LN formation is initiated during embryogenesis.

Recently a model describing the development of PP was proposed (Honda et al., 2001). It was shown that lymphoid lineage IL-7R⁺CD3⁻ cells considered to be PP inducers express CXC chemokine receptor 5 (CXCR5) and are capable of producing membrane-associated LTα1β2 heterotrimer (Honda et al., 2001), while in contrast, mesenchymal lineage vascular cell adhesion mole-

cule (VCAM)-1$^+$ and intercellular adhesion molecule (ICAM)-1$^+$ PP organizers express LTβR (Honda et al., 2001). Following stimulation signals provided via IL-7R, PP inducers express LTα1β2 to activate PP organizers via LTβR, while PP organizers produce chemokines such as B lymphocyte chemoattractant (BLC) and EBV-induced molecule 1 ligand chemokine (ELC) to stimulate PP inducers via CXCR5 and the CC chemokine receptor (CCR) 7 (Honda et al., 2001). The reciprocal interaction between inducer and organizer cells via chemokine and cytokine receptors is essential for the formation of PP, and the loss of any part of either of the signaling programs is sufficient to disrupt secondary lymphoid tissue development, as evidenced by the loss of PP in LTβR$^{-/-}$ and IL-7Rα$^{-/-}$ mice (Futterer et al., 1998; Adachi et al., 1998). *Aly/aly* mice which have defective NIK function also fit this paradigm, as recent analyses have established that NIK is essential to the mediation of TNFR family signal transduction, including that of LTβR (Nakano et al., 1996; Shinkura et al., 1999; Yin et al., 2001). Thus, *aly/aly* mice lack PP and LN (Miyawaki et al., 1994) since the NIK mutation inhibited reciprocal interaction between PP inducers and organizers via LTα1β2 and LTβR. Further evidence in support of this model comes from studies showing that mice which lack the CD3$^-$CD4$^+$CD45$^+$ inducer cells due to genetic deletion of the Id2 or RORγ genes also completely lack PP and LN (Sun et al., 2000; Yokota et al., 1999).

In this study, we have examined and compared the contribution of tissue organogenesis-associated cytokine signals provided via IL-7R, LTβR, and NIK for the formation of NALT and PP. Our novel findings constitute direct evidence that CD3$^-$CD4$^+$CD45$^+$ cells can provide an IL-7R-, LTα1β2/LTβR-, and NIK-independent tissue organogenesis pathway for the initiation of a secondary lymphoid tissue development. Thus, the formation of NALT differs markedly from that of other lymphoid tissues such as PP and LN.

Results

Postnatal Development of NALT

In normal mice, NALT is a bell-shaped accumulation of lymphoid cells (Figures 1C and 2A). NALT-associated HEV express PNAd, an addressin phenotype distinct from the mucosal addressin cell adhesion molecules (MAdCAM)-1$^+$ that characterizes the HEV of PP (Csencsits et al., 1999). To determine when NALT developed, we immunohistologically analyzed PNAd in wild-type mice of various ages. NALT formation, indicated by the expression of PNAd and an accumulation of mononuclear cells, was not observed during embryogenesis or in newborn nasal tissue (Figure 1A, and data not shown), whereas PP with associated HEV were already developed (Figure 1E). Instead, PNAd$^+$ HEV with associated lymphocytes were detected bilateral manner in nasal tissue beginning at 1 week postpartum (Figures 1B and 1D) and was strongly expressed in 8-week-old mice (Figure 1C), as compared with isotype control mAb (Figure 1H). As expected, the size of PP tissue continued to increase with the increasing age of the mice (Figures 1E–1G). These findings suggested that the initiation of tissue organogenesis is chronologically different in NALT and PP.

Development of NALT in Secondary Lymphoid Tissue-Deficient Mice

To investigate the involvement of lymphoid tissue organogenesis-related signals provided by IL-7/IL-7R, LTα1β2/LTβR, and NIK in the formation of NALT, we next examined mice lacking PP and/or LN: IL-7Rα$^{-/-}$, LTα$^{-/-}$, LTβ$^{-/-}$, *aly/aly* mice, and mice treated in utero with LTβR-Ig fusion protein. NALT was detected in all PP null or PP/LN null mouse strains (Figures 2B–2E, 2G). However, the size of NALT was smaller in IL-7Rα$^{-/-}$, LTα$^{-/-}$, LTβ$^{-/-}$, and *aly/aly* mice compared with NALT of wild-type mice (Figure 2). Furthermore, we compared the NALT formation in mice treated in utero with that of those treated at birth with LTβR-Ig. PP-deficient mice that had been treated in utero with LTβR-Ig were observed to form NALT (Figure 2E). Since our study demonstrated that the initiation of NALT formation occurred 1 week after birth (Figure 1), it was formally possible that in utero-administered fusion protein might drop below a minimum effective dose prior to the onset of NALT development postnatally. Therefore, we next administered LTβR-Ig fusion protein into newborn mice and observed that they too developed NALT (Figure 2F). These results suggest that the induction of NALT formation requires a cytokine signaling cascade independent from those of PP since tissue organogenesis signals provided by IL-7R, LTα1β2/LTβR, and NIK pathways are not essential for the initial stage of NALT development.

Detection of PNAd$^+$ HEV in NALT of PP-Deficient Mice

PNAd$^+$ HEV was detected in the NALT of IL-7Rα$^{-/-}$, LTα$^{-/-}$, LTβ$^{-/-}$, and *aly/aly* mice as well as in that of mice treated with LTβR-Ig in utero and at birth (Figure 3). PNAd expression on NALT in these mice further confirmed that NALT formation is independent of the cytokine pathways that trigger PP and LN formation. However, the levels of PNAd expression in the NALT of these PP- and/or LN-deficient mice seemed to be lower than in wild-type mice (Figures 3A and 3C). Although the expression of PNAd was influenced by nasal immunization with CT in LTα$^{-/-}$ mice, the level was still low when compared with wild-type mice (Figures 3A and 3D). These results suggest that at least a part of the PNAd expression in NALT is regulated under IL-7R and LTα1β2/LTβ R-NIK signals.

Role of L-Selectin/PNAd for the Formation of NALT

Inasmuch as the molecular interaction of L-selectin and PNAd has been shown to be a key step for the migration of lymphoid cells into NALT (Csensits at al., 1999), we thought it important to examine whether NALT formation is influenced by the blockade of this adhesion molecule interaction. To directly address the role of L-selectin in the development of NALT, we analyzed NALT formation in L-selectin$^{-/-}$ mice. Gross histology revealed that though NALT was present in L-selectin$^{-/-}$ mice (Figures 3J and 3K), it was smaller than that of normal control mice. Further, the treatment of C57BL6/c mice with anti-PNAd mAb (MECA79) resulted in the reduction of the size of NALT (Figures 3L and 3M). These results indicate the possible contribution of other adhesion molecules that might compensate for the homing of NALT lymphocytes in L-selectin$^{-/-}$ mice and anti-PNAd mAb-treated

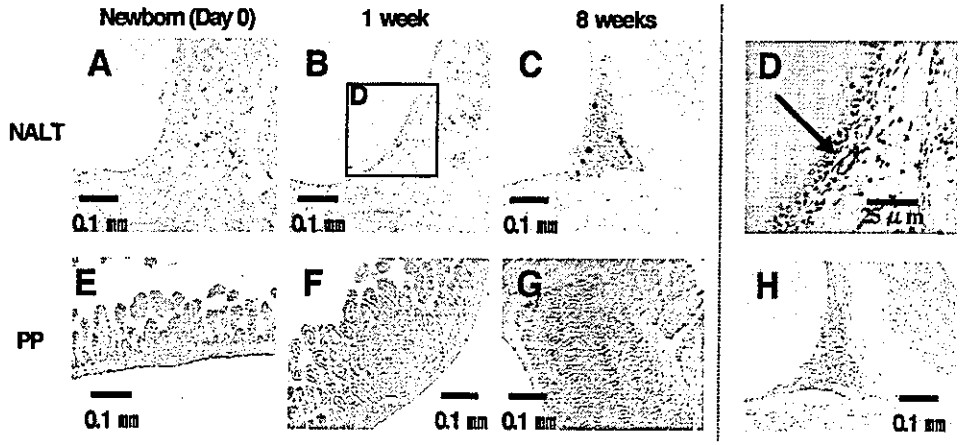

Figure 1. Chronological Analysis and Comparison of the Development of NALT and PP

(A–D) Fixed tissue sections were stained with MECA 79 (rat anti-mouse PNAd mAb) to detect NALT HEV, followed by counterstaining with hematoxylin. (A) Nasal tissue from newborn mice (day 0) with no PNAd-expressing HEV. (B) The NALT anlagen from 1-week-old mice with small accumulation of lymphoid cells around single PNAd-expressing HEV in the nasal tissue. (C) 8-week-old murine NALT with numerous PNAd-expressing HEV. (D) Enlargement of the NALT anlagen of the 1-week-old mice from Figure 2B. Arrows point to PNAd-expressing HEV. (E–G) Fixed tissue sections were HE stained for the detection of PP. (E) PP in the intestine from newborn mice (day 0). (F) PP in the intestine of 1-week-old mice. (G) PP in the intestine of 8-week-old mice.
(H) Isotype matched irrelevant Ab (rat IgM, R4-22; PharMingen) reacted with nasal tissue of 8-week-old mice.

mice. However, these findings do not diminish the importance of PNAd/L-selectin interaction for the entry of lymphocytes into NALT.

Characterization of Lymphoid Cells Isolated from NALT

Since tissue organogenesis of NALT was maintained in PP null mice, we next characterized lymphocytes isolated from the NALT of LTα$^{-/-}$, *aly/aly*, and strain-matched wild-type mice. Flow cytometry analysis of NALT mononuclear cells in the wild-type and *aly/+* mice revealed populations of B220^{+} B cells (70%–80%) and CD3^{+} T cells (14%–20%; Table 1), findings in agreement with those of our previous study (Hiroi et al., 1998). In contrast, a higher frequency (51%) of CD3^{+} T cells ($p < 0.05$) was noted in NALT lymphocytes isolated from LTα$^{-/-}$ than from wild-type mice (19%; Table1). When NALT lymphocytes isolated from *aly/+* and *aly/aly* mice were compared, the frequency of B and T cells in *aly/+* and *aly/aly* mice was similar to that of wild-type and LTα$^{-/-}$ NALT, respectively. The frequency of CD11c^{+} dendritic cells was higher in NALT isolated from *aly/aly* mice ($p < 0.05$) than in control *aly/+* NALT (Table 1). Despite the alteration in the frequency of B and T cells

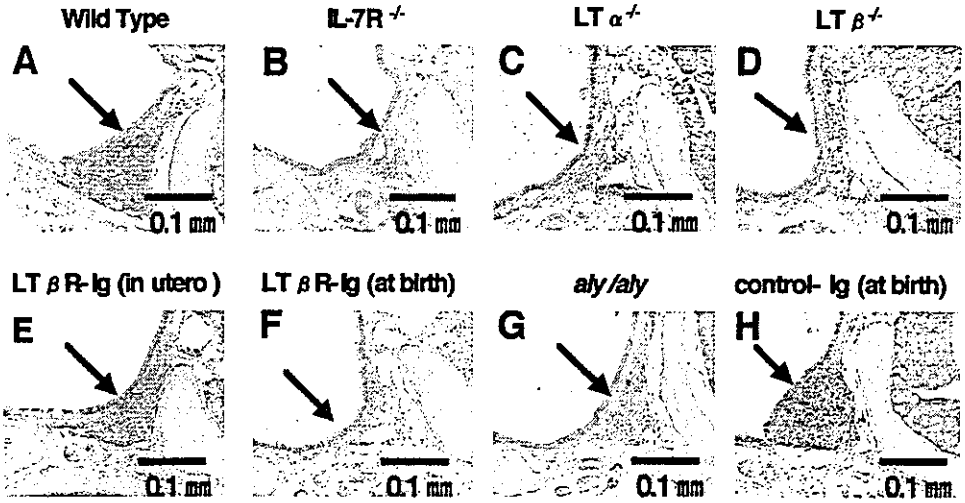

Figure 2. Development of NALT in Secondary Lymphoid Tissue-Deficient Mice

Paraffin sections with HE staining were prepared from 8-week-old mice.
(A) NALT of wild-type (WT) mice. (B) NALT of IL-7Rα$^{-/-}$ mice. (C) NALT of LTα$^{-/-}$mice. (D) NALT of LTβ$^{-/-}$mice. (E) NALT of mice treated with LTβR-Ig fusion protein in utero. (F) NALT of mice treated with LTβR-Ig fusion protein at birth. (G) NALT of *aly/aly* mice. (H) NALT of mice treated with control-Ig at birth. Arrows point to NALT.

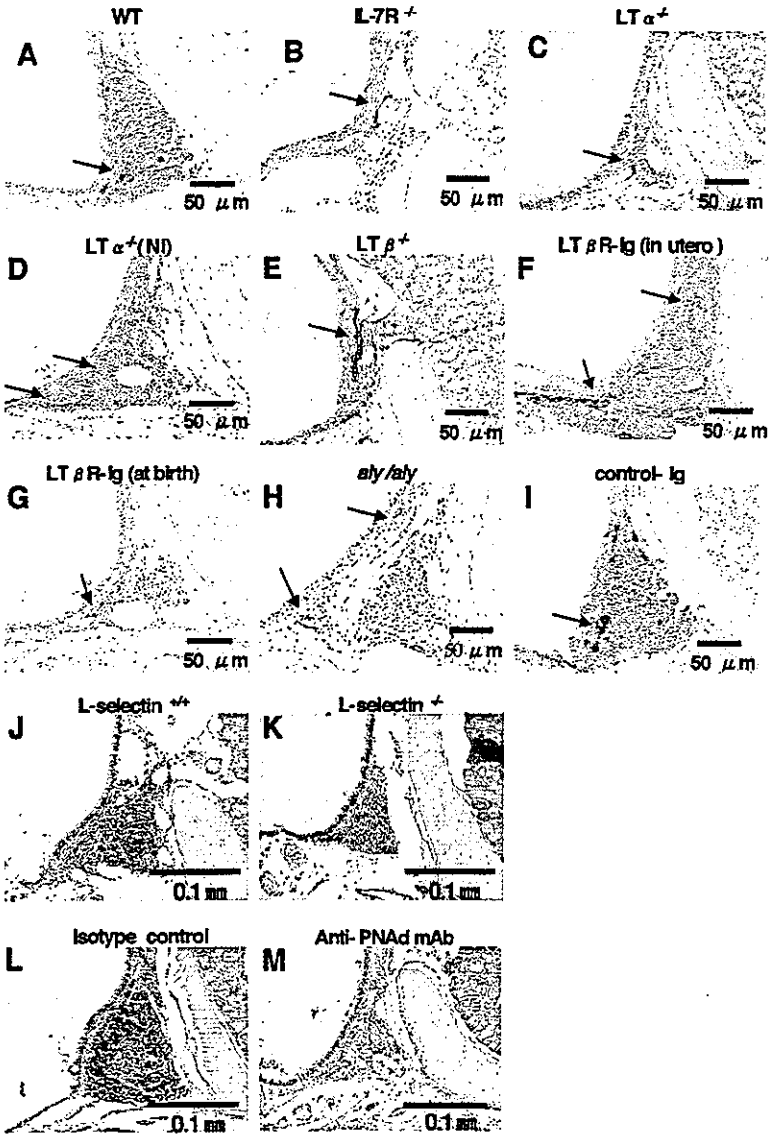

Figure 3. Role of PNAd and L-Selectin for the Development of NALT

PNAd$^+$ HEV was detected in NALT of mice lacking PP and/or LN (A–I). NALT was developed in L-selectin$^{-/-}$ mice and wild-type mice treated with anti-PNAd mAb (J–M).

(A–I) All fixed tissue sections isolated from 8-week-old mice were stained with MECA 79 (rat anti-mouse PNAd mAb) for the detection of HEV, followed by counterstaining with hematoxylin. Arrows point to PNAd-expressing HEV. (A) NALT of wild-type (WT) mice. (B) NALT of IL-7Rα$^{-/-}$ mice. (C) NALT of LTα$^{-/-}$ mice. (D) NALT of LTα$^{-/-}$ mice after nasal immunization (NI) with CT, as described in Experimental Procedures. (E) NALT of LTβ$^{-/-}$mice. (F) NALT of mice treated with LTβR-Ig fusion protein in utero. (G) NALT of mice treated with LTβR-Ig fusion protein at birth. (H) NALT of *aly/aly* mice. (I) NALT of mice treated with control-Ig at birth.

(J–M) Paraffin sections with HE staining were prepared from background mice (J) and L-selectin$^{-/-}$ mice (K). A similar preparation was made for isotype control Ab- (L) and mAb anti-PNAd (M)-treated WT mice. For the treatment, WT mice were systemically treated with mAb anti-PNAd (MECA-79) or isotype control (rat IgM) once per week for 5 consecutive weeks.

in NALT lymphocytes from wild-type and PP-deficient mice, the ratio of CD4/CD8 in CD3$^+$ T cells did not change among these different mice groups (Table 1). Although there was some alteration in the ratio of B and T cells isolated from the NALT of wild-type and PP null mice, our findings demonstrate that lymphoid cells, including B cells, T cells and DC, accumulate in the NALT of PP-deficient mice (LTα$^{-/-}$ and *aly/aly*).

Development of CD3$^-$CD4$^+$CD45$^+$ Cells in Infant NALT

CD3$^-$CD4$^+$CD45$^+$ cells are considered critical for secondary lymphoid tissue development (Honda et al., 2001; Sun et al., 2000; Yokota et al., 1999). Thus, we next searched for such cells in NALT isolated from infant mice. FACS analysis revealed the presence of CD3$^-$CD4$^+$CD45$^+$ cells in NALT of 2-week-old wild-type (0.32%; 20.8 × 10^3/mouse) and LTα$^{-/-}$mice (0.22%; 4.40 × 10^3/mouse) (Figure 4). A similar population of CD3$^-$CD4$^+$CD45$^+$ cells (1.90%; 1.43 × 10^4/mouse) was found in the intestines of E18 embryos (Figure 4). It was interesting that a small population of CD3$^-$CD4$^+$CD45$^+$ cells was still present in infant NALT because these cells were hardly detectable in peripheral blood after birth (Mebius et al., 1997). This finding was further confirmed by immunohistological analysis. In 10-day-old wild-type and LTα$^{-/-}$ mice, small numbers of CD3$^-$CD4$^+$ cells were noted in the bilateral NALT anlagen (Figures 4A–4C). Thus, CD3$^-$CD4$^+$ inducer cells were found at the initiation site of NALT organogenesis.

The Id2 Gene Is an Essential Molecule for the Organogenesis of NALT

The accumulation of CD3$^-$CD4$^+$CD45$^+$ cells in NALT anlagen suggested that these cells might be involved in NALT organogenesis. Therefore, we investigated nasal tissues in Id2$^{-/-}$ mice that lack this cell population (Yo-

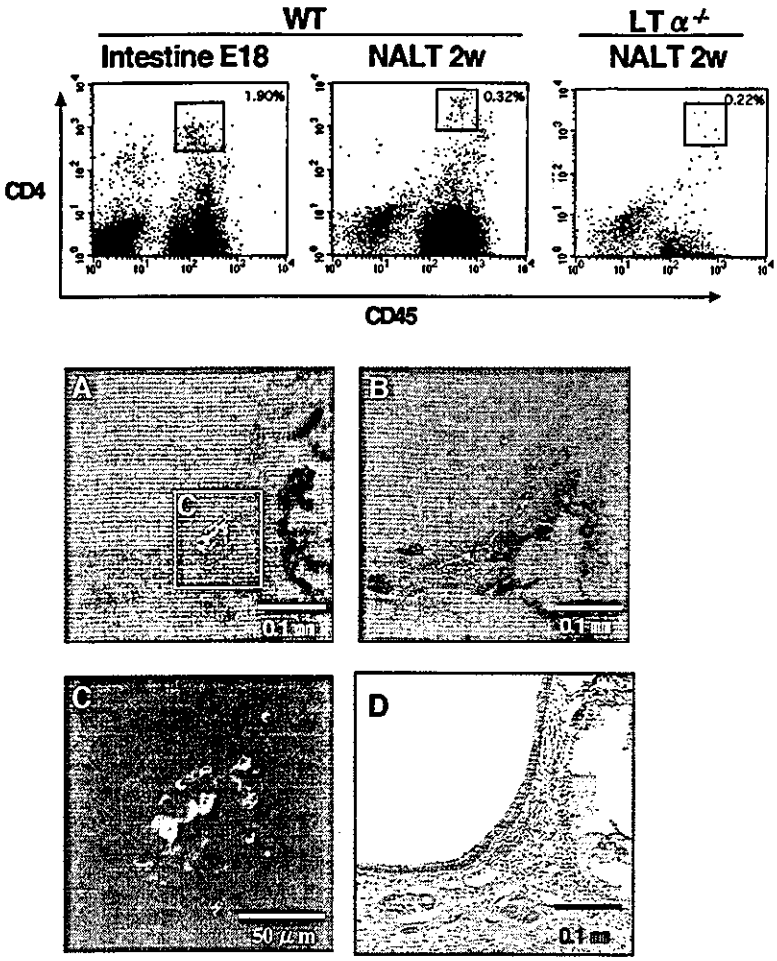

Figure 4. Presence of Inducer $CD3^-CD4^+CD45^+$ Cells in Infant NALT

Lymphoid cells were isolated from the intestines of E18 embryos and from NALT of 2-week-old wild-type (WT) and $LT\alpha^{-/-}$ mice. Cells were then first stained with FITC-anti-CD45, PE-anti-CD4, and biotin-anti-CD3 mAbs, and then with streptavidin-APC. The percentage of $CD3^-CD4^+CD45^+$ cells was determined by flow cytometry after gating for the CD3 negative fraction.

(A) The accumulation of $CD3^-CD4^+$ cells was detected in bilateral NALT anlage in 10-day-old WT mice and (B) $LT\alpha^{-/-}$ mice. (C) Enlargement of the NALT anlage of 10-day-old mice from (A). Fixed tissue was stained with FITC-anti-CD3 and PE-CD4 mAbs, and then examined by confocal microscopy. (D) A serial section of (A) was also stained by HE. A control experiment using confocal analysis was performed using spleen of adult WT mice stained with the same combination of the fluorescence-conjugated mAbs (data not shown).

kota et al., 1999) and found that $Id2^{-/-}$ mice were deficient in NALT (Figures 5A and 5B). Furthermore, PNAd expression was not observed in the $Id2^{-/-}$ mice, whereas this addressin was found in NALT of wild-type littermates (Figures 5D and 5E). In the next experiment, we nasally immunized $Id2^{-/-}$ mice with CT. Although the size of NALT was enlarged after the nasal immunization of $LT\alpha^{-/-}$ mice with CT (Figures 3C and 3D), there were no sign of NALT development or PNAd expression on vessels in the nasal tissue of nasally immunized $Id2^{-/-}$ mice (Figures 5C and 5F). These results further confirmed our finding that the development of NALT is defective in $Id2^{-/-}$ mice. The analysis of $Id2^{-/-}$ mice indicates that a population of inducer cells, i.e., $CD3^-CD4^+CD45^+$ cells, is involved in the development of NALT and that the organogenesis of NALT, like that of PP and LN, depends on the helix-loop-helix inhibitor Id2 (Yokota et al., 1999).

Table 1. Analysis of Lymphocytes in NALT Isolated from PP Null and Wild-Type Mice

	Total Numbers of Cell Isolated ($\times 10^4$)	Surface Marker-Positive Cells (%) (Number of Positive Cells $\times 10^3$)			Ratio of T Cell Subset
		CD3	B220	CD11c	CD4/CD8
Wild-type	26.5 ± 1.0	19.1 ± 1.5 (50.7 ± 4.6)	69.9 ± 4.6 (185.0 ± 10.9)	1.9 ± 0.5 (5.4 ± 1.3)	1.7 ± 0.2
$LT\alpha^{-/-}$	1.8 ± 0.3	51.2 ± 3.5* (7.2 ± 1.7*)	31.3 ± 4.7* (5.5 ± 0.9*)	2.9 ± 1.0 1.4 ± 0.1*)	1.9 ± 0.2
aly/+	4.2 ± 1.4	13.5 ± 1.0 (5.8 ± 1.4)	77.1 ± 5.2 (31.5 ± 4.1)	1.2 ± 0.2 (0.5 ± 0.2)	1.9 ± 0.2
aly/aly	3.3 ± 0.2	57.1 ± 4.0* (18.9 ± 1.9*)	31.1 ± 12.1* (10.2 ± 4.0*)	7.6 ± 0.8* (0.25 ± 0.2)	2.1 ± 0.1

Lymphocytes were isolated from NALT of PP deficient- and wild-type control-mice. Cells were then stained with FITC-, PE-, or APC-conjugated mAbs specific for CD3, CD4, CD8, CD11c, and B220 as described in Experimental Procedures. The percentage and the number of positive cells were determined by flow cytometry and represented mean ± SEM from three different experiments.
*$p < 0.05$.

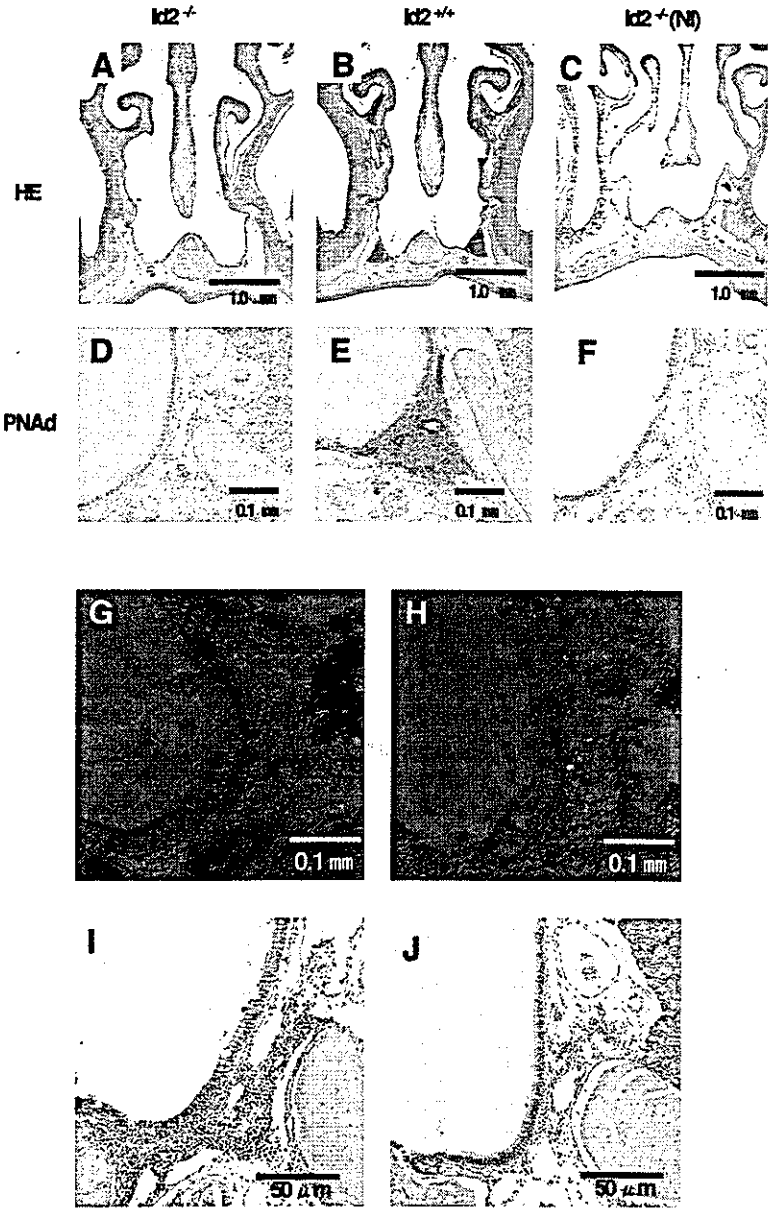

Figure 5. Essential Role of Id2 and $CD3^-CD4^+CD45^+$ Cells for the NALT Organogenesis

Id2 deficiency resulted in the lack of NALT formation (A–F). NALT organogenesis was induced in $Id2^{-/-}$ mice by the adoptive transfer of fetal liver or $CD3^-CD4^+CD45^+$ cells (G–J).

(A–C) Fixed tissue sections were stained with HE.

(D–F) Tissue sections were stained with MECA79, followed by counterstaining with hematoxylin. (A) NALT was absent in the nasal tissue of $Id2^{-/-}$mice. (B) NALT was intact in $Id2^{+/+}$ littermates. (C) NALT was not developed in $Id2^{-/-}$mice nasally immunized (NI) with CT. (D) PNAd expression of HEV in the nasal tissue was not detected in $Id2^{-/-}$mice. (E) HEV of NALT in $Id2^{+/+}$ littermates normally expressed PNAd. (F) PNAd expression was not developed in $Id2^{-/-}$mice after nasal immunization of CT.

(G and H) Fixed tissue was stained with FITC-anti-CD3 and PE-CD4 mAbs and then examined by confocal microscopy. (G) $CD3^-CD4^+$ cells were absent in the nasal tissue of $Id2^{-/-}$ infant mice. (H) $CD3^-CD4^+$ cells were found to have accumulated in the nasal tissue of $Id2^{-/-}$ infant mice 7 days after the adoptive transfer with fetal liver cells.

(I and J) The same tissues stained by HE. In these experiments, each group containing three $Id2^{-/-}$ mice was adoptively transferred with fetal liver cells or $CD3^-CD4^+CD45^+$ cells. Development of NALT-like structure was noted in all of these adoptively transferred mice. (I) A NALT-like structure was observed to have developed in $Id2^{-/-}$ mice 7 weeks after the adoptive transfer with fetal liver cells. (J) A NALT-like structure was noted in $Id2^{-/-}$ mice transferred with $CD3^-CD4^+CD45^+$ cells.

Organogenesis of NALT in $Id2^{-/-}$ Mice after Adoptive Transfer with Fetal Liver or $CD3^-CD4^+CD45^+$ Cells

In order to clarify the role of $CD3^-CD4^+CD45^+$ cells for the induction of NALT development, we first performed an adoptive transfer experiment of fetal liver cells from $Id2^{+/+}$ mice into $Id2^{-/-}$ mice (Figures 5G–5J). Seven days after the transfer of fetal liver cells into $Id2^{-/-}$ newborn mice, $CD3^-CD4^+$ cells had migrated into the site of NALT formation (Figures 5G and 5H) and, seven weeks after transfer, a NALT-like structure was detected (Figure 5I). Furthermore, the adoptive transfer of $CD3^-CD4^+CD45^+$ cells isolated from fetal intestine of wild-type mice into $Id2^{-/-}$ newborn mice led to the initiation of NALT-like structure in $Id2^{-/-}$ mice (Figure 5J). These findings are a direct demonstration that $CD3^-CD4^+CD45^+$ cells from fetal liver function to initiate lymphoid tissue organogenesis (e.g., NALT). However, the lymphoid structure induced by the adoptive transfer of $CD3^-CD4^+CD45^+$ cells was smaller than that induced by the adoptive transfer with fetal liver cells (Figures 5I and 5J), suggesting that additional cell types contribute to the full development of NALT tissue.

Discussion

This study provides persuasive and direct evidence that the mechanism of cytokine- and cytokine receptor-mediated organogenesis in NALT is distinct from that in PP and LN. First, NALT was shown to develop in various circumstances which are known to cause PP and LN deficiency, as for example, in $LT\alpha^{-/-}$, $LT\beta^{-/-}$, *aly/aly* mice, and mice treated in utero with LTβR-Ig. Since NALT tissue organogenesis begins after birth, we also treated mice with LTβR-Ig postnatally to ensure that the antagonist was present during the initial stage of NALT formation. NALT was still detected in mice

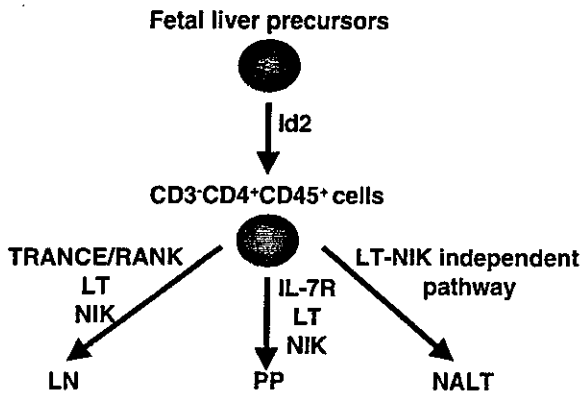

Figure 6. A Summary of the Proposed Organogenesis of NALT, PP, and LN

In the case of LN and PP, $CD3^-CD4^+CD45^+(IL\text{-}7R\alpha^+)$ cells are considered to be the inducer of secondary lymphoid tissue. Id2 is indispensable for the induction and the differentiation of the inducer cells from the fetal liver precursors. Following activation via IL-7R, these $CD3^-CD4^+CD45^+$ cells express $LT\alpha1\beta2$ heterotrimer, which then binds to LTβR for the subsequent signal transduction via NIK for the expression of necessary adhesion molecules and/or chemokines. The accumulation of lymphoid cells is induced by these homing-related molecules (e.g., PP). The development of $CD3^-CD4^+CD45^+$ cells in NALT also requires Id2, but the initiation of NALT organogenesis is independent of IL-7R, $LT\alpha1\beta2/LT\beta R$, and NIK signaling. It is not yet known which cytokines and corresponding receptors fill the roles of the IL-7R, $LT\alpha1\beta2/LT\beta R$, and NIK signaling pathways for the formation of NALT.

treated at birth with LTβR-Ig. LTβR is a critical signaling molecule for stromal cell activation at the site of PP and LN formation via signals transduced to NF-κB through NIK (Fagarasan et al., 2000; Honda et al., 2001; Yin et al., 2001). The ability of NALT to form in the absence of LTβR signaling and NIK function suggests that a unique signal exists to trigger NALT organogenesis (Figure 6). It was also interesting to note that the gross architecture of NALT varied among LT-deficient mice, mice treated in utero with LTβR-Ig, and mice treated after birth with LTβR-Ig, suggesting that the LTβR cytokine signaling cascade contributes to the maturation of cellularity and to the gross development of NALT.

IL-7Rα signaling also is essential for the initiation of PP organogenesis, since IL-7R engagement is thought to be required for $CD3^-CD4^+CD45^+$ cells to express $LT\alpha1\beta2$ (Adachi et al. 1998; Yoshida et al., 1999). NALT development in $IL\text{-}7R\alpha^{-/-}$ mice is further evidence that the signaling axis that induces NALT organogenesis is distinct from that which triggers PP formation. Although IL-7R signaling was not essential for the initiation of NALT organogenesis, the maturation of NALT structure was incomplete in $IL\text{-}7R^{-/-}$ mice when compared with wild-type mice (Figures 2 and 3). Other known signaling axes for secondary lymphoid organ formation include the TRANCE/RANK pathway for LN development (Kim et al., 2000). The potential role of this pathway for NALT genesis is not yet known.

$CD3^-CD4^+CD45^+$ cells expressing $LT\alpha1\beta2$ heterotrimers have been implicated as an inducer cell population for secondary lymphoid tissue formation including PP (Sun et al., 2000; Yokota et al., 1999). The observation that NALT development is distinct from that of PP led us to ask if the $CD3^-CD4^+CD45^+$ cells played a role in NALT organogenesis. The helix-loop-helix inhibitor Id2 is a key regulatory factor for the differentiation of $CD3^-CD4^+CD45^+$ cells from stem cells, and the absence of these cells in $Id2^{-/-}$ mice correlates with the loss of PP and LN (Yokota et al., 1999). We have now demonstrated that NALT is deficient in $Id2^{-/-}$ mice (Figure 5). $CD3^-CD4^+CD45^+$ cells have been shown to be derived from fetal liver cells in vivo (Mebius et al., 2001; Yoshida et al., 2001). Therefore, the adoptive transfer of fetal liver cells or $CD3^-CD4^+CD45^+$ cells from $Id2^{+/+}$ wild-type mice into $Id2^{-/-}$ newborn mice resulted in the migration of $CD3^-CD4^+CD45^+$ cells to the site of NALT formation and in the formation of NALT-like structure (Figure 5). This constitutes a direct, functional demonstration that $CD3^-CD4^+CD45^+$ cells deliver an organogenic signal to the site of secondary lymphoid organ formation such as NALT. The formation of other secondary lymphoid tissues absent from $Id2^{-/-}$ mice was not achieved using this protocol, as the transfer of cells occurred after birth, that is, after the developmental window during which LN and PP formation is initiated (data not shown). Thus, Id2-regulated $CD3^-CD4^+CD45^+$ cells are the common-ancestor (or inducer) cells for the organogenesis of NALT as well as PP, although the $CD3^-CD4^+CD45^+$ cells do not use the IL-7R-mediated $LT\alpha1\beta2/LT\beta R$ cytokine signaling cascade for the onset of secondary lymphoid tissue formation in the upper respiratory tract. Our current effort is aimed at identifying the critical signaling cytokine and corresponding receptor used by $CD3^-CD4^+CD45^+$ cells for the initiation of NALT development.

It was interesting to note that PNAd expression was not observed in these NALT-like structures of $Id2^{-/-}$ mice adoptively transferred with fetal liver cells or $CD3^-CD4^+CD45^+$ cells (data not shown). These results suggest that additional factors including cytokine, chemokine, and/or adhesion molecule might be necessary for the maturation of NALT in $Id2^{-/-}$ mice adoptively transferred with fetal liver cells or $CD3^-CD4^+CD45^+$ cells. The finding that NALT is formed in $L\text{-selectin}^{-/-}$ mice and wild-type mice treated with anti-PNAd mAb also supports the hypothesis that multiple signals contribute to the NALT formation and subsequent development (Figure 3). Addressins were similarly absent from LN induced to form in $LT\alpha^{-/-}$ mice (Rennert et al., 1998), likewise suggesting that LTα and/or LTαβ regulate(s) PNAd (and MAdCAM-1) expression in developing NALT. Furthermore, the NALT-like structure of $Id2^{-/-}$ mice adoptively transferred with $CD3^-CD4^+CD45^+$ cells was smaller than the NALT formed after fetal liver cell transfer. This result suggests that an additional population of inducer/organizer type cells might be necessary for the formation of mature NALT in addition to $CD3^-CD4^+CD45^+$ cells.

There was a chronological difference between lymphoid development in the nasal tract and the intestine (Figure 1). NALT was not present during embryogenesis, whereas it is known that LN development begins as early as E11 and PP development on E16.5 in the embryonic mesentery and intestine, respectively (Rennert et al., 1997; Yoshida et al., 1999). Further, we could not detect $PNAd^+$ HEV, an important adhesion molecule for the recruitment of lymphocytes to NALT (Csencsits et al.,

1999), in the nasal tract of embryonic mice. NALT and PNAd-positive HEV were not present until 7 days after birth. MAdCAM-1 is expressed on the HEV of gut-associated lymphoid tissues, such as PP in mice (Berlin et al., 1993), and is identified as early as E16.5 at the site of PP organogenesis (Hashi et al., 2001). HEV of LN anlagen similarly expresses MAdCAM-1 starting early in development, with strong expression in newborn mice (Mebius et al., 1996). The expression of MAdCAM-1 is reportedly very low or absent from the HEV of adult NALT (Csencsits et al., 1999), and we found that the HEV of infant NALT (e.g., 7 days old) did not express MAdCAM-1 (data not shown). Thus, NALT formation is chronologically and immunohistochemically distinct from that of PP and LN. Adhesion molecule or addressin expression is thought to be a critical early step in the organogenesis of PP (VCAM-1, MAdCAM-1) and PLN (MAdCAM-1) (Adachi et al., 1997; Hashi et al., 2001; Kim et al., 2000; Mebius et al., 1996). These results suggest that PNAd expression may play a similar role in the development of NALT.

In keeping with a recent report, we found that NALT continued to express PNAd in the adult mouse (Csencsits et al., 1999). We found PNAd expressed on the HEV of NALT in adult LTα$^{-/-}$, LTβ$^{-/-}$, IL-7Rα$^{-/-}$, and *aly/aly* mice, although the intensity of PNAd expression was somewhat lower in these mice than in wild-type mice. The TNF receptor family regulates the expression of several adhesion (or homing) molecules and chemokines for the homing of lymphocytes to secondary lymphoid tissues and inflammatory lesions (Cuff et al., 1999), and these signals are likely transduced in part through NIK (Fagarasan et al., 2000; Nakano et al., 1996; Yin et al., 2001). Our results suggest that the expression of PNAd in NALT is in part regulated by LTα1β2/LTβR- and NIK-associated signaling events. Since the PNAd expression defect is particularly pronounced in LTα$^{-/-}$ mice, an additional role for LTα3/TNF-R signaling should be considered.

Based on the results generated in the present study, two possibilities can be proposed to explain the differences between the mechanisms responsible for the organogenesis of NALT and PP. First, NALT formation could be preprogrammed to initiate IL-7R-, LTα1β2/LTβR-, and NIK-independent tissue organogenesis signaling events after nativity. Alternatively, NALT development may depend on triggering signals provided by inhaled environmental antigens after birth. Taken together, it is likely that NALT organogenesis is preprogrammed to be inaugurated following nativity via an undefined cytokine and corresponding receptor signaling cascade, and inhaled antigens may initiate or accelerate the signals in this cascade. In support of this proposal, PP formation is complete within a few days after birth (and exposure to luminal antigens), although the basic architecture of the tissue is formed during the gestational period (e.g., E15.5) (Hashi et al., 2001).

In summary, our results demonstrate that the formation of NALT is initiated independently of IL-7R, LTα1β2/LTβR, and NIK, but nonetheless relies on the presence of common inducer (ancestor) cells which are CD3$^-$CD4$^+$CD45$^+$ cells. In the case of LN and PP formation, these cells are triggered to express LTα1β2 heterotrimer, which activates LTβR$^+$ stromal organizer cells causing them to express VCAM-1, ICAM-1, or MAdCAM-1 (Honda et al., 2001). Although the organogenesis of NALT requires Id2 and its associated inducer CD3$^-$CD4$^+$CD45$^+$ cells, as does that of PP and LN, the initiation of NALT organogenesis is independent of IL-7R, LTα1β2/LTβR, and NIK signaling cascades (Figure 6). Unique, but not yet identified, molecules may be involved in the lymphoid tissue organogenesis of NALT. Thus, multiple cytokine receptor signaling pathways seem to be important for the organization of cellularity and for the gross development of NALT. Elucidation of the details of this unique signaling axis for NALT organogenesis, including the cytokines, chemokines, and adhesion molecules involved, may further our understanding of the alternative events that trigger secondary lymphoid tissue organogenesis.

Experimental Procedures

Mice

C57BL/6J Jcl mice and *aly/aly* mice (ALY/Nsc Jcl-*aly/aly*) were obtained from Japan Clea Co. (Tokyo, Japan). LTα$^{-/-}$ (C57BL/6) mice and L-selectin$^{-/-}$ (B6/129S) mice were obtained from Jackson Laboratories (Bar Harbor, ME). IL-7Rα$^{-/-}$ (129/Ola×C57BL/6) mice were kindly provided by Immunex Corp. (Seattle, WA) (Peschon et al., 1994). Id2$^{-/-}$ (129/Sv) mice were generated as described (Yokota et al., 1999). These strains were maintained in conventional housing at the Experimental Animal Facility of the Research Institute for Microbial Diseases, Osaka University (Osaka, Japan). The nasal tissue of LTβ$^{-/-}$ mice was kindly provided by Dr. R. Flavell (Koni et al., 1997), Biogen Inc (Cambridge, MA). Pregnant wild-type mice were injected intravenously with 200 μg of LTβR-Ig fusion protein on gestational days 14 and 17. In some experiments, the peritoneal cavity of newborn mice was injected with LTβR-Ig fusion protein or control IgG (50 μg/mouse) according to the method described previously (Yamamoto et al., 2000). LTβR-Ig fusion protein and control IgG were also prepared as described elsewhere (Rennert et al., 1997, 1998).

Wild-type mice were treated with anti-PNAd mAb (50 μg/mouse, MECA-79, BD PharMingen, SanDiego, CA) or isotype control (rat IgM, PharMingen) once per week for 5 consecutive weeks.

Histology and Immunohistochemistry

The heads and the intestines of the mice were fixed in 4% paraformaldehyde. Adult nasal tissues isolated from 6- to 8-week-old mice were decalcified in EDTA solution for 10 days, and all tissues were embedded in paraffin. Frontal sections of the nasal tissues (5 μm) and intestinal sections with PP (5 μm) were stained with hematoxylin/eosin (HE). For immunohistochemical staining, deparaffinated sections (5 μm) were incubated with anti-PNAd mAb (MECA-79; PharMingen) according to the method described previously (Csencsits et al., 1999). The sections were then incubated with biotinylated secondary Ab (ZYMED, San Francisco, CA) and exposed to avidin-biotin-peroxidase complex (Vector Laboratories, Burlingame, CA). After color development with diaminobenzidine, the sections were counterstained with hematoxylin.

For confocal microscopic analysis, the nasal tissues from 7-day-old mice were fixed in 4% paraformaldehyde and rapidly frozen in OCT embedding medium (Sakura Finetechnical Co., Ltd., Tokyo, Japan). Cryostat sections (5 μm) were prepared and stained with FITC-anti-CD3ε (145-2C11; PharMingen) and PE-anti-CD4 (RM4-5; PharMingen) mAbs for 1 hr at room temperature. Histological analysis was performed using confocal microscopy (Bio-Rad Laboratories Inc., Hercules, CA).

Nasal Immunization

LTα$^{-/-}$ and Id2$^{-/-}$ mice were immunized nasally with 10 μl of PBS containing CT (5 μg/mouse; Sigma Chemical, St. Louis, MO) once per week for 3 consecutive weeks. Nasal tissues were collected 7 days after final immunization.

Isolation and FACS Analysis of Mononuclear Cells

Mononuclear cells from NALT were isolated as described (Asanuma et al., 1995; Hiroi et al., 1998). In brief, the mononuclear cells were isolated by gentle teasing through stainless steel screens, and FACS analysis was performed (Hiroi et al., 1994, 1995). The mononuclear cell preparation was pretreated with anti-CD16/CD32 FcR mAb (2.4G2) and then stained with the appropriate fluorescence-conjugated anti-CD3ε (145-2C11), anti-CD4 (RM4-5), anti-CD8 (53-6.7), anti-B220 (RA3-6B2), anti-CD45 (30-F11), and anti-CD11c mAb (HL3) (all from PharMingen). Flow cytometry analysis and cell isolations were then performed using FACSCalibur and FACS Vantage (Becton Dickinson, San Jose, CA), respectively.

Adoptive Transfer Experiment of Fetal Liver Cells or $CD3^-CD4^+CD45^+$ Cells

Fetal liver cells were collected from E16 $Id2^{+/+}$ embryos, and $CD3^-CD4^+CD45^+$ cells were isolated from the fetal intestine (E18) of $Id2^{+/+}$ mice by using FACS Vantage (Becton Dickinson), as previously described, with some modifications (Yoshida et al., 2001). Isolated cells were cultured in medium containing RPMI 1640, 10% FBS, 50 μg/ml penicillin G, 50 U/ml streptomycin, 100 ng/ml IL-7 (Genzyme, Cambridge, MA), and 100 ng/ml stem cell factor (R&D Systems, Minneapolis, MN) in order to activate these cells (Yoshida et al., 1999). After 1 day of culture, these fetal liver cells (1.0×10^5) or $CD3^-CD4^+CD45^+$ cells (1.0×10^3) were injected into the peritoneal cavity of $Id2^{-/-}$ newborn mice. The nasal tissues obtained from 7-day-old $Id2^{-/-}$ mice adoptively transferred with fetal liver cells were analyzed by confocal microscopy (Bio-Rad Laboratories Inc., Hercules, CA). Histological analysis was also performed for the nasal tissues of 7- to 8-week-old $Id2^{-/-}$ mice adoptively transferred with fetal liver cells or $CD3^-CD4^+CD45^+$ cells.

Acknowledgments

This work was supported by a Grant-in-Aid for COE Research from the Ministry of Education, Science, Sports, and Culture of Japan; the Ministry of Health, Labor, and Welfare of Japan; and the Japanese Human Science Foundation. We thank the members of the Mucosal Immunology Group of Osaka University for their critical comments. We also thank Noriko Kitagaki for her technical help.

References

Adachi, S., Yoshida, H., Kataoka, H., and Nishikawa, S.-I. (1997). Three distinctive steps in Peyer's patch formation of murine embryo. Int. Immunol. *9*, 507–514.

Adachi, S., Yoshida, H., Honda, K., Maki, K., Saijo, K., Ikuta, K., Saito, T., and Nishikawa, S.-I. (1998). Essential role of IL-7 receptor alpha in the formation of Peyer's patch anlage. Int. Immunol. *10*, 1–6.

Asanuma, H., Inaba, Y., Aizawa, C., Kurata, T., and Tamura, S. (1995). Characterization of mouse nasal lymphocytes isolated by enzymatic extraction with collagenase. J. Immunol. Methods *187*, 41–51.

Berlin, C., Berg, E.L., Briskin, M.J., Andrew, D.P., Kilshaw, P.J., Holzmann, B., Weissman, I.L., Hamann, A., and Butcher, E.C. (1993). Alpha 4 beta 7 integrin mediates lymphocyte binding to the mucosal vascular addressin MAdCAM-1. Cell *16*, 185–190.

Crowe, P.D., VanArsdale, T.L., Walter, B.N., Ware, C.F., Hession, C., Ehrenfels, B., Browning, J.L., Din, W.S., Goodwin, R.G., and Smith, C.A. (1994). A lymphotoxin-beta-specific receptor. Science *264*, 707–710.

Csencsits, K.L., Jutila, M.A., and Pascual, D.W. (1999). Nasal-associated lymphoid tissue: phenotypic and functional evidence for the primary role of peripheral node addressin in naive lymphocyte adhesion to high endothelial venules in a mucosal site. J. Immunol. *163*, 1382–1389.

Cuff, C.A., Sacca, R., and Ruddle, N.H. (1999). Differential induction of adhesion molecule and chemokine expression by LTα3 and LTαβ in inflammation elucidates potential mechanisms of mesenteric and peripheral lymph node development. J. Immunol. *162*, 5965–5972.

De Togni, P., Goellner, J., Ruddle, N.H., Streeter, P.R., Fick, A., Mariathasan, S., Smith, S.S., Carlson, R., Shornick, L.P., Strauss-Schoenberger, J., et al. (1994). Abnormal development of peripheral lymphoid organs in mice deficient in lymphotoxin. Science *264*, 703–707.

Fagarasan, S., Shinkura, R., Nogaki, T., Ikuta, K., Tashiro, K., and Honjo, T. (2000). Alymphoplasia (aly)-type nuclear factor kappa B-inducing kinase (NIK) causes defects in secondary lymphoid tissue chemokine receptor signaling and homing of peritoneal cells to the gut-associated lymphatic tissue system. J. Exp. Med. *191*, 1477–1486.

Futterer, A., Mink, K., Luz, A., Kosco-Vilbois, M.H., and Pfeffer, K. (1998). The lymphotoxin beta receptor controls organogenesis and affinity maturation in peripheral lymphoid tissues. Immunity *9*, 59–70.

Hashi, H., Yoshida, H., Honda, K., Fraser, S., Kubo, H., Awane, M., Takabayashi, A., Nakano, H., Yamaoka, Y., and Nishikawa, S.-I. (2001). Compartmentalization of Peyer's patch anlagen before lymphocyte entry. J. Immunol. *166*, 3702–3709.

Hiroi, T., Fujihashi, K., McGhee, J.R., and Kiyono, H. (1994). Characterization of cytokine-producing cells in mucosal effector sites: $CD3^+$Tcells of Th1 and Th2 type in salivary gland-associated tissue. Eur. J. Immunol. *24*, 2653–2658.

Hiroi, T., Fujihashi, K., McGhee, J.R., and Kiyono, H. (1995). Polarized Th2 cytokine expression by both mucosal γδ and αβ T cells. Eur. J. Immunol. *25*, 2743–2751.

Hiroi, T., Iwatani, K., Iijima, H., Kodama, S., Yanagita, M., and Kiyono, H. (1998). Nasal immune system: distinctive Th0 and Th1/Th2 type environments in murine nasal-associated lymphoid tissues and nasal passage, respectively. Eur. J. Immunol. *28*, 3346–3353.

Honda, K., Nakano, H., Yoshida, H., Nishikawa, S., Rennert, P., Ikuta, K., Tamechika, M., Yamaguchi, K., Fukumoto, T., Chiba, T., et al. (2001). Molecular basis for hemotopoietic/mesenchymal interaction during initiation of Peyer's patch organogenesis. J. Exp. Med. *193*, 621–630.

Imaoka, K., Miller, C.J., Kubota, M., McChesney, M.B., Lohman, B., Yamamoto, M., Fujihashi, K., Someya, K., Honda, M., McGhee, J.R., et al. (1998). Nasal immunization of nonhuman primates with simian immunodeficiency virus p55gag and cholera toxin adjuvant induces Th1/Th2 help for virus specific immune responses in reproductive tissues. J. Immunol. *161*, 5952–5958.

Jeong, K.I., Suzuki, H., Nakayama, H., and Doi, K. (2000). Ultrastructural study on the follicle-associated epithelium of nasal-associated lymphoid tissue in specific pathogen-free (SPF) and conventional environment-adapted (SPF-CV) rat. J. Anat. *196*, 443–451.

Kim, D., Mebius, R.E., MacMicking, J.D., Jung, S., Cupedo, T., Castellanos, Y., Rho, J., Wong, B.R., Josien, R., Kim, N., et al. (2000). Regulation of peripheral lymph node genesis by the tumor necrosis factor family member TRANCE. J. Exp. Med. *192*, 1467–1478.

Koni, P.A., Sacca, R., Lawton, P., Browning, J.L., Ruddle, N.H., and Flavell, R.A. (1997). Distinct roles in lymphoid organogenesis for lymphotoxins α and β revealed in lymphotoxin β-deficient mice. Immunity *6*, 491–500.

Kuper, C.F., Hemeleers, D.M., Bruijntjes, J.P., van der Ven, I., Biewenga, J., and Sminia, T. (1990). Lymphoid and non-lymphoid cells in nasal-associated lymphoid tissue (NALT) in the rat. An immuno- and enzyme-histochemical study. Cell Tissue Res. *259*, 371–377.

Kuper, C.F., Koornstra, P.J., Hameleers, D.M., Biewenga, J., Spit, B.J., Duijvestijin, A.M., van Breda Vriesman, P.J., and Sminia, T. (1992). The role of nasopharyngeal lymphoid tissue. Immunol. Today *13*, 219–224.

Kurono, Y., Yamamoto, M., Fujihashi, K., Kodama, S., Suzuki, M., Mogi, G., McGhee, J.R., and Kiyono, H. (1999). Nasal immunizaton induces *Haemophilus influenzae*-specific Th1 and Th2 responses with mucosal IgA and systemic IgG antibodies for protective immunity. J. Infect. Dis. *180*, 122–132.

Mebius, R.E., Streeter, P.R., Michie, S., Butcher, E.C., and Weissman, I.L. (1996). A developmental switch in lymphocyte homing receptor and endothelial vascular addressin expression regulates lymphocyte homing and permits $CD4^+CD3^-$ cells to colonize lymph nodes. Proc. Natl. Acad. Sci. USA *93*, 11019–11024.

Mebius, R.E., Rennert, P., and Weissman, I.L. (1997). Developing lymph nodes collect $CD4^+CD3^-$ $LT\beta^+$ cells that can differentiate to

APC, NK cells, and follicular cells but not T or B cells. Immunity *7*, 493–504.

Mebius, R.E., Miyamoto, T., Christensen, J., Domen, J., Cupedo, T., Weissman, I.L., and Akashi, K. (2001). The fetal liver counterpart of adult common lymphoid progenitors gives rise to all lymphoid lineages, CD45(+)CD4(+)CD3(−) cells, as well as macrophages. J. Immunol. *166*, 6593–6601.

Miyawaki, S., Nakamura, Y., Suzuka, H., Koba, M., Yasumizu, R., Ikehara, S., and Shibata, Y. (1994). A new mutation, *aly*, that induces a generalized lack of lymph nodes accompanied by immunodeficiency in mice. Eur. J. Immunol. *24*, 429–434.

Nakano, H., Oshima, H., Chung, W., Williams-Abbott, L., Ware, C.F., Yagita, H., and Okumura, K. (1996). TRAF5, an activator of NF-κB and putative signal transducer for the lymphotoxin-beta receptor. J. Biol. Chem. *271*, 14661–14664.

Peschon, J.J., Morrissey, P.J., Grabstein, K.H., Ramsdell, F.J., Maraskovsky, E., Gliniak, B.C., Park, L.S., Ziegler, S.F., Williams, D.E., and Ware, C.B. (1994). Early lymphocyte expansion is severely impaired in interleukin 7 receptor-deficient mice. J. Exp. Med. *180*, 1955–1960.

Rennert, P.D., Browning, J.L., Mebius, R., Mackay, F., and Hochman, P.S. (1996). Surface lymphotoxin alpha/beta complex is required for the development of peripheral lymphoid organs. J. Exp. Med. *184*, 1999–2006.

Rennert, P.D., Browning, J.L., and Hochman, P.S. (1997). Selective disruption of lymphotoxin ligands reveals a novel set of mucosal lymph nodes and unique effects on lymph node cellular organization. Int. Immunol. *9*, 1627–1639.

Rennert, P.D., James, D., Mackay, F., Browning, J.L., and Hochman, P.S. (1998). Lymph node genesis is induced by signaling through the lymphotoxin β receptor. Immunity *9*, 71–79.

Shimoda, M., Nakamura, T., Takahashi, Y., Asanuma, H., Tamura, S., Kurata, T., Mizuochi, T., Azuma, N., Kanno, C., and Takemori, T. (2001). Isotype-specific selection of high affinity memory B cells in nasal-associated lymphoid tissue. J. Exp. Med. *194*, 1597–1607.

Shinkura, R., Kitada, K., Matsuda, F., Tashiro, K., Ikuta, K., Suzuki, M., Kogishi, K., Serikawa, T., and Honjo, T. (1999). Alymphoplasia is caused by a point mutation in the mouse gene encoding NF-κB-inducing kinase. Nat. Genet. *22*, 74–77.

Sun, Z., Unutmaz, D., Zou, Y., Sunshine, M.J., Pierani, A., Brenner-Morton, S., Mebius, R.E., and Littman, D.R. (2000). Requirement for RORγ in thymocyte survival and lymphoid organ development. Science *288*, 2369–2373.

Yamamoto, M., Rennert, P., McGhee, J.R., Kweon, M.-N., Yamamoto, S., Dohi, T., Otake, T., Bluethmann, H., Fujihashi, K., and Kiyono, H. (2000). Alternate mucosal immune system: organized Peyer's patches are not required for IgA responses in the gastrointestinal tract. J. Immunol. *164*, 5184–5191.

Yanagita, M., Hiroi, T., Kitagaki, N., Hamada, S., Ito, H., Shimauchi, H., Murakami, S., Okada, H., and Kiyono, H. (1999). Nasopharyngeal-associated lymphoreticular tissue (NALT) immunity: fimbriae-specific Th1 and Th2 cell-regulated IgA responses for the inhibition of bacterial attachment to epithelial cells and subsequent inflammatory cytokine production. J. Immunol. *162*, 3559–3565.

Yin, L., Wu, L., Wesche, H., Arthur, C.D., White, J.M., Goeddel, D.V., and Schreiber, R.D. (2001). Defective lymphotoxin-beta receptor-induced NF-kappa B transcriptional activity in NIK-deficient mice. Science *291*, 2162–2165.

Yokota, Y., Mansouri, A., Mori, S., Sugawara, S., Adachi, S., Nishikawa, S.-I., and Gruss, P. (1999). Development of peripheral lymphoid organs and natural killer cells depends on the helix-loop-helix inhibitor Id2. Nature *397*, 702–706.

Yoshida, H., Honda, K., Shinkura, R., Adachi, S., Nishikawa, S., Maki, K., Ikuta, K., and Nishikawa, S.-I. (1999). IL-7 receptor α^+ $CD3^-$ cells in the embryonic intestine induces the organizing center of Peyer's patches. Int. Immunol. *11*, 643–655.

Yoshida, H., Kawamoto, H., Santee, S.M., Hashi, H., Honda, K., Nishikawa, S., Ware, C.F., Katsura, Y., and Nishikawa, S.-I. (2001). Expression of α4β7 integrin defines a distinct pathway of lymphoid progenitors committed to T cells, fetal intestinal lymphotoxin producer, NK, and dendritic cells. J. Immunol. *167*, 2511–2521.

Note Added in Proof

Since this manuscript was submitted, Randall and colleagues published similar findings on the independence of LTα for the organogenesis of NALT (Harmsen et al., 2002 [J. Immunol.]).

IL-15-Dependent Activation-Induced Cell Death-Resistant Th1 Type CD8$\alpha\beta^+$NK1.1$^+$ T Cells for the Development of Small Intestinal Inflammation[1]

Noriyuki Ohta,*† Takachika Hiroi,* Mi-Na Kweon,* Naotoshi Kinoshita,* Myoung Ho Jang,* Tadashi Mashimo,† Jun-Ichi Miyazaki,‡ and Hiroshi Kiyono[2]*§

To clarify the role of IL-15 at local sites, we engineered a transgenic (Tg) mouse (T3^b-IL-15 Tg) to overexpress human IL-15 preferentially in intestinal epithelial cells by the use of T3^b-promoter. Although IL-15 was expressed in the entire small intestine (SI) and large intestines of the Tg mice, localized inflammation developed in the proximal SI only. Histopathologic study revealed reduced villus length, marked infiltration of lymphocytes, and vacuolar degeneration of the villus epithelium, beginning at ~3–4 mo of age. The numbers of CD8$^+$ T cells, especially CD8$\alpha\beta^+$ T cells expressing NK1.1, were dramatically increased in the lamina propria of the involved SI. The severity of inflammation corresponded to increased numbers of CD8$\alpha\beta^+$NK1.1$^+$ T cells and levels of production of the Th1-type cytokines IFN-γ and TNF-α. Locally overexpressed IL-15 was accompanied by increased resistance of CD8$\alpha\beta^+$ NK1.1$^+$ T cells to activation-induced cell death. Our results suggest that chronic inflammation in the SI in this murine model is mediated by dysregulation of epithelial cell-derived IL-15. The model may contribute to understanding the role of CD8$^+$ T cells in human Crohn's disease involving the SI. *The Journal of Immunology,* **2002, 169: 460–468.**

Interleukin-15 and IL-2 share many molecular, biological, and immunologic features (1, 2). Both are members of the 4α-helix bundle cytokine family, use IL-2Rβ chain and common γ-chain for their action in T cells, and have similar functional activities for the activation and growth of T and NK cells. Despite the similarities between these two cytokines, they differ dramatically in their expression levels at cellular sites and the regulation levels of synthesis and secretion (3–6). IL-2 is produced by activated T cells and controlled predominantly at the levels of mRNA transcription and stabilization, whereas the control of IL-15 expression is much more complex, with regulation at the levels of transcription, translation, and intracellular trafficking (7–9).

IL-15 mRNA is widely expressed in macrophages as well as various nonlymphoid tissues and cells, such as placenta, skeletal muscle, kidney, lung, fibroblasts, and epithelial cells (9, 10). Because the discovery that intestinal epithelial cells (IECs)[3] can produce IL-15 in mice, rats, and humans, a focus of research in mucosal immunity has been the possible role of IL-15 in the mucosal intranet between IEC and intestinal intraepithelial lymphocytes (IEL) (11–13). In addition, our previous study showed that IL-15/IL-15R interaction is important in humoral aspects of mucosal immunity such as IgA production. IL-15Rα chain is expressed on mucosal B-1 but not B-2 cells, and IEC-derived IL-15 may be a selective regulatory factor for the terminal differentiation of IgA-committed B-1 cells into IgA-producing cells (14).

IL-15 is a key regulatory cytokine, which supports innate immune cell development, activation, and homeostasis. Translation of IL-15 expression is strictly regulated at multiple distinct steps to mediate appropriate levels of the cytokine expression (4–8). Removal of these negative control mechanisms in an integrated fashion may lead to a major increase in IL-15 synthesis, resulting in loss of homeostasis between innate and acquired immunity. Multiple negative regulatory features controlling IL-15 expression may be required because of the potency of IL-15 as an inflammatory cytokine; if unrestrictedly expressed, IL-15, with its capacity to provide pleiotropic effects on various kinds of effector lymphoid cells, might initiate serious disorders such as autoimmune diseases.

IL-15 reportedly is overexpressed in rheumatoid arthritis (15, 16) and allograft rejection (17), and IL-15-recruited and activated autoreactive T cells in the synovial membrane have led to TNF-α secretion in synovial fluids (15, 16). Targeted treatment for the blockade of IL-15R elements, including IL-15Rβ chain and the common γ-chain, has inhibited the development of some experimental immunologic diseases, including collagen-induced arthritis (18) and allograft rejection (19, 20). Thus, IL-15 likely plays a critical role in the immunopathology of chronic inflammation. In the mucosa-associated inflammation of the chronic inflammatory bowel diseases, expression of IL-15 mRNA was found to be increased in the inflamed intestinal tissues of ulcerative colitis (21–23), and in Crohn's disease, expression of IL-15 was increased in intestinal macrophages (24).

In the present study, we have developed a novel in vivo IL-15 overexpression system for the murine intestine. Localized overexpression of intestinal IL-15 led to the development of a unique subset of activation-induced cell death (AICD)-resistant Th1-type

*Department of Mucosal Immunology, Research Institute for Microbial Diseases, Osaka University, and Departments of †Anesthesiology, and ‡Nutrition and Physiological Chemistry, Osaka University Medical School, Osaka, Japan; and §Division of Mucosal Immunolgy, Department of Microbiology and Immunology, Institute of Medical Science, University of Tokyo, Tokyo, Japan

Received for publication December 27, 2001. Accepted for publication April 29, 2002.

The costs of publication of this article were defrayed in part by the payment of page charges. This article must therefore be hereby marked *advertisement* in accordance with 18 U.S.C. Section 1734 solely to indicate this fact.

[1] This work was supported by the Center of Excellence and Scientific Research at the Frontier from the Ministry of Education, Science, Sports and Culture, and grants from the Ministry of Health, Labor, and Welfare, and Japanese Human Science Foundation.

[2] Address correspondence and reprint requests to Dr. Hiroshi Kiyono, Department of Mucosal Immunology, Research Institute for Microbial Diseases, Osaka University, 3-1 Yamadaoka, Suita, Osaka 565-0871, Japan. E-mail address: kiyono@biken.osaka-u.ac.jp

[3] Abbreviations used in this paper: IEC, intestinal epithelial cell; IEL, intraepithelial lymphocyte; AICD, activation-induced cell death; SP, signal peptide; MP, mature protein; RGP, rat glucagon promoter; MLN, mesenteric lymph node; LP, lamina propria; APN, allophycocyanin; Tg, transgenic; WT, wild type; SI, small intestine; LI, large intestine.

0022-1767/02/$02.00

$CD8\alpha\beta^+$ $NK1.1^+$ T cells and the induction of aberrant immunologic reactions in the small intestine (SI), but not the large intestine (LI).

Materials and Methods

DNA construct

To develop intestinal IL-15 transgenic (Tg) mice, a $T3^b$-promoter system was used (Fig. 1*A*; Ref. 25). Complementary DNAs encoding the human IL-2 signal peptide (SP), the human IL-15 mature protein (MP) coding sequence, and the FLAG epitope tag (Eastman Kodak, Rochester, NY) were amplified by PCR and fused by use of standard PCR-based methods as described previously (7). The rat glucagon promoter (RGP)-IL-2SP/IL-15 MP/FLAG plasmid contained the RGP, the IL-2SP/IL-15/FLAG cDNA, and rabbit-β globin gene sequences from the second exon to the polyadenylation signal. The $T3^b$-IL-2SP/IL-15 MP/FLAG transgene was constructed by replacing the RGP promoter of the RGP-IL-2SP/IL-15 MP/FLAG plasmid with the 2.8-kb *SphI-Hin*dIII $T3^b$ promoter region obtained from the $T3^b$ gene cloned into the pUC18 plasmid. Finally, a 5.5-kb *SphI-XhoI* $T3^b$-IL-2SP/IL-15/FLAG DNA fragment was purified and used for microinjection (Fig. 1*A*).

Generation of $T3^b$-IL-2SP/IL-15 MP/FLAG Tg mice

BDF1, C57BL/6Cr, and MCH-ICR mice purchased from Japan SLC (Shizuoka, Japan) were used throughout this study. Mice were maintained under specific pathogen-free conditions in the animal facility at The Research Institute for Microbial Diseases (Osaka University, Osaka, Japan). The transgene was microinjected into the pronuclei of BDF1-fertilized eggs as described (26). For screening of founder mice, tail DNA was isolated by the SDS-proteinase K method. Founders were genotyped by PCR using specific primers for the transgene. The oligonucleotide 5′-GCTGGTTAT TGTGCTGCTTC-3′ was used as a forward primer, and 5′-CATCTCCG GACTCAAGTGAA-3 was used as a backward primer. The PCR conditions were initially 94°C for 3 min, and 30 cycles of amplification, each cycle consisting of 94°C for 1 min, 59°C for 1 min, and 72°C for 1 min followed by an extension for 10 min at 72°C.

Semiquantitative RT-PCR for measurement of IL-2SP/IL-15 MP/FLAG mRNA

Total RNA was extracted from various tissues by using the guanidine thiocyanate procedure. DNase digestion of extracted RNA was performed before cDNA synthesis. One microgram of total RNA was reverse transcribed into cDNA using SuperScript II RT (Life Technologies, Gaithersburg, MD). To apply the same amount of synthesized cDNA from various tissues, the amounts of synthesized cDNA labeled with digoxigenin were measured with a chemiluminescent image analyzer (Molecular Imager System; Bio-Rad, Hercules, CA). PCR amplification of 10 ng of cDNA for each sample was performed with the GeneAmp PCR System 9700 (PerkinElmer/Cetus, Branchburg, NJ). The oligonucleotide primers used for the IL-2SP/IL-15 MP/FLAG mRNA were: forward, 5′-TCCTGTCTT GCATTGCACTAAG-3′; reverse, 5′-CACATTCTTTGCATCCAGATT-3′. After heating at 94°C for 2 min, cDNA were amplified for 35 cycles, each cycle consisting of 95°C for 0 s, 55°C for 30 s, and 72°C for 30 s. The amplified products were separated by electrophoresis in 1.8% agarose gel and were visualized with ethidium bromide (1 μg/ml).

Western blot analysis

The lysates of various organs were loaded directly onto 8–16% gradient gels (Tris-HCL; Bio-Rad). Proteins were electrophoresed under denaturing conditions and electroblotted to nitrocellulose membranes at 60 V for 4 h at 4°C. Membranes were blocked overnight with 1% blocking reagent (Roche Diagnostics, Mannheim, Germany) in PBS containing 0.5% Tween 20 (PBS-T) and then incubated for 2 h with mouse anti-human IL-15 mAb (clone 34593.11; R&D Systems, Minneapolis, MN) or anti-FLAG M2 mAb (Sigma-Aldrich, St. Louis, MO) diluted in PBS-T plus 2% blocking reagent. After washing of the gels with PBS-T, protein was detected by use of an ImmunoStar kit for mouse (Wako Biochemicals, Osaka, Japan) according to the manufacturer's instructions.

Isolation of mononuclear cells

The spleen and mesenteric lymph nodes (MLNs) were aseptically removed, and single-cell suspensions were prepared by a standard mechanical disruption procedure, as described previously (27). Mononuclear cells of intestinal lamina propria (LP) were prepared by an enzymatic dissociation method using type IV collagenase (Sigma-Aldrich; Ref. 27). After removal of PP and MLN, the intestine was opened longitudinally, washed thoroughly, and cut into small fragments. Epithelial cells and IEL were removed from intestinal tissue by incubating in RPMI 1640 containing 0.5 mM EDTA and 2% FCS. The specimens were then minced and added to RPMI 1640 containing collagenase at 37°C incubation. Mononuclear cells were then isolated by use of a discontinuous density gradient procedure (40 and 75%) with Percoll (Amersham Pharmacia Biotech, Uppsala, Sweden). For the isolation of IEC, a discontinuous density gradient (25, 40, and 75%) was also used. The cells that layered between the 40 and 25% interface were collected as IEC (28).

Abs and reagents

PE-conjugated anti-TCRβ (H57-597), anti-CD8α (53-6.7), anti-CD8β.2 (53-5.8), anti-CD62L (MEL-14), anti-CD44 (IM7), anti-NK1.1 (PK136), anti-CD25 (7DA), CD69 (H1.2F3), anti-CD122 (TM-β1), anti-IFN-γ (XMG1.2), anti-TNF-α (MP6-XT22), and anti-IL-2 (JES6-5H4), FITC-conjugated anti-CD4 (RM4-5), anti-CD8β (53-5.8), anti-Ly-6C (AL-21), and anti-CD25 (7DA), and allophycocyanin (APN)-conjugated anti-CD8α (53-6.7) and anti-TCR-β (H57-597) were purchased from BD PharMingen (San Diego, CA). Biotin-conjugated anti-human IL-15 (34593.11) was obtained from R&D Systems.

Histologic analysis

The en bloc-fixed gastrointestinal tract was dissected into stomach, jejunum, ileum, SI, LI, and rectum. Tissue specimens were fixed in 4% paraformaldehyde and embedded in paraffin. Sections were cut and then stained with H&E.

Flow cytometric analysis

For analysis of surface markers of lymphocytes isolated from either MLN or the LP of the SI, cells were stained with PE-, FITC-, and APN-conjugated mAbs. To block FcR-mediated binding of the mAb, anti-FcR mAb (2.4G2; BD PharMingen) was added. All incubation steps were performed at 4°C for 30 min. To detect biotin-conjugated mAb, cells were stained with APN-conjugated streptavidin after incubation with a primary mAb. The stained cells were analyzed by a FACSCalibur flow cytometer (BD Biosciences, Mountain View, CA) and data were analyzed by using CellQuest software (BD Biosciences). Dead cells positively stained with propidium iodide were gated out. For intracellular cytokine staining, cells from the MLN and LP were cultured with complete RPMI 1640 medium containing 10% FBS, 5 μM 2-ME, 10 U/ml penicillin, 100 μg/ml streptomycin in 12-well flat-bottom plates coated with anti-CD3 mAb (145-2C11; 10 μg/ml; BD PharMingen) for 6 h at 37°C in the presence of 5 μg/ml brefeldin A (Sigma-Aldrich). After being stained for surface Ags, cells were subjected to intracellular cytokine staining, using Cell Fixation/Permeabilization kits (BD PharMingen).

AICD

Populations of apoptotic cells in freshly isolated LP lymphocytes were detected by staining with annexin V and propidium iodide, using the Annexin V FITC Apoptosis Detection kit I (BD PharMingen) and then analyzed by flow cytometry. For flow cytometric TUNEL staining analysis, freshly isolated LP lymphocytes were analyzed by APO-DIRECT kit (BD PharMingen).

Data analysis

Data were expressed as mean ± SE and evaluated by the Mann-Whitney *U* test for unpaired samples, using a Statview II statistical program (SAS Institute, Cary, NC) designed for the Macintosh computer. Values of $p < 0.05$ were assumed to be statistically significant.

Results

Selective expression of human IL-15 in the intestine of $T3^b$-IL-15 Tg mice

Human IL-15 was expressed under the control of the $T3^b$ promoter, which supports specific transcription in IEC (Fig. 1*A*). Eight founder animals were maintained by mating to C57BL/6 mice. For analysis of the tissue specificity of transgene expression, total RNA was isolated from various tissues of Tg and wild-type (WT) mice and subjected to IL-15-specific semiquantitative RT-PCR analysis (Fig. 1*B*). Tg IL-2SP/IL-15 MP/FLAG mRNA was expressed selectively in the gastrointestinal tract, i.e., SI and LI; but

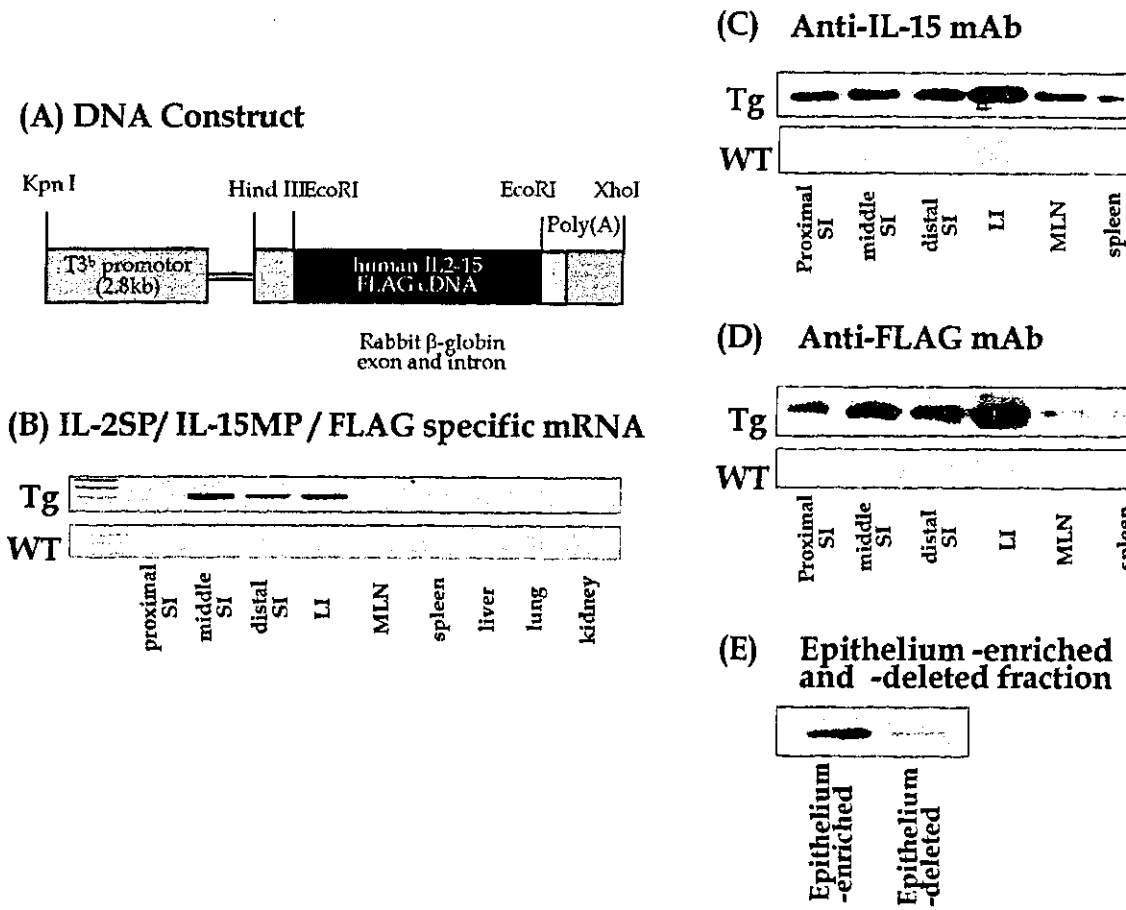

FIGURE 1. Construction of T3^b-IL-15 Tg mice for the development of intestinal inflammation. *A*, Intestinal epithelium-specific expression was accomplished by use of the T3^b-promoter. *B*, RT-PCR analysis of various tissues from T3^b-IL-15 Tg mice demonstrated that human IL-15 mRNA was selectively expressed in the gut (proximal, middle, and distal SI; and LI). Various tissue lysates were analyzed by Western blot, using anti-hIL-15 mAb (*C*) or anti-FLAG mAb (*D*) to detect protein levels of human IL-15. The expression of IL-15 in IEC-enriched and -deleted fractions of the SI was compared (*E*). Non-Tg WT mice were used as negative controls.

not in other tissues, i.e., MLN, spleen, liver, and lung. IL-15 production by IEC was confirmed also at the protein level by Western blotting analysis (Fig. 1, *C–E*). Abundant IL-15 protein was present in the SI and LI and in MLN. IL-15 was also detected, but in lower amounts, in spleen, liver, and lung of the T3^b-IL-15 Tg mice, probably reflecting the presence of IL-15 in serum, at the level of ~100 pg/ml. That IL-15 was most abundantly expressed in the intestinal tract indicated that this newly established Tg animal could be used as a model for examining the role of IL-15 in the intestinal immune system.

Intestinal epithelium-specific overexpression of IL-15 causes intestinal inflammation

In two separate Tg lines, designated T3^b-IL-15 Tg-3-8 and T3^b-IL-15 Tg-10-7, macroscopic and histologic signs of intestinal inflammation developed, beginning at about 3 mo of age (Fig. 2, *A* and *B*). In this report, the findings in the T3^b-IL-15 Tg-3-8 line are presented. Macroscopically, the jejunum and proximal ileum were severely affected, with swelling of the tissue (Fig. 2*A*) and sometimes, hemorrhage. In contrast, the LI was not affected (Fig. 2*A*).

Histologic analysis of the gastrointestinal tract also revealed profound pathologic changes in the SI but not the LI of the T3^b-IL-15 Tg mice at 6 mo of age (Figs. 2, *B* and *C*). Massive infiltration of mononuclear cells into the LP of the jejunum and proximal ileum (Fig. 2, *B, a* and *b*), as well as Paneth cell deletion, hyperemia, and crypt elongation were observed. Neither the stomach nor terminal ileum was affected. Furthermore, no pathological changes were detected in the LI (Fig. 2*C*). Infiltrated areas of the SI had vacuolar degeneration of the epithelial cells, especially at the villus tips, and occasionally in the crypts (Fig. 2*Bc*). In contrast to the situation in many previous models of intestinal inflammation, neither ulceration nor prominent influx of granulocytes was noted in the Tg mice (Fig. 2*Bd*). We did find that the ratio of villus to crypt height was 6.4:1 in WT compared with 2.1:1 in the Tg mice, a finding suggesting that IL-15 can directly regulate the development of IEC or that neighboring mucosal T cells activated by IL-15 can subsequently affect the IEC development (29). The pathologic changes in the SI became worse as the disease progressed (3 mo (Fig. 2*B, e–g*) vs 6 mo (Fig. 2*B, a–d*)). In addition, the yield of cells from the MLN and intestinal LP, but not from the IEL compartment, was significantly increased in the Tg mice compared with the WT mice. This increase of lymphocytes was not detected in other lymphoid tissues, such as the cervical lymph nodes. The cumulative incidence of mucosal inflammation in the T3^b-IL-15 Tg-3-8 mice was nearly 100% at 6 mo of age, and most of the diseased mice eventually died despite being reared under specific pathogen-free conditions. These results indicate that the overexpression of IL-15 resulted in increased lymphoid cell numbers selectively in the mucosa-associated tissues, and this increase was associated with gross intestinal disease.

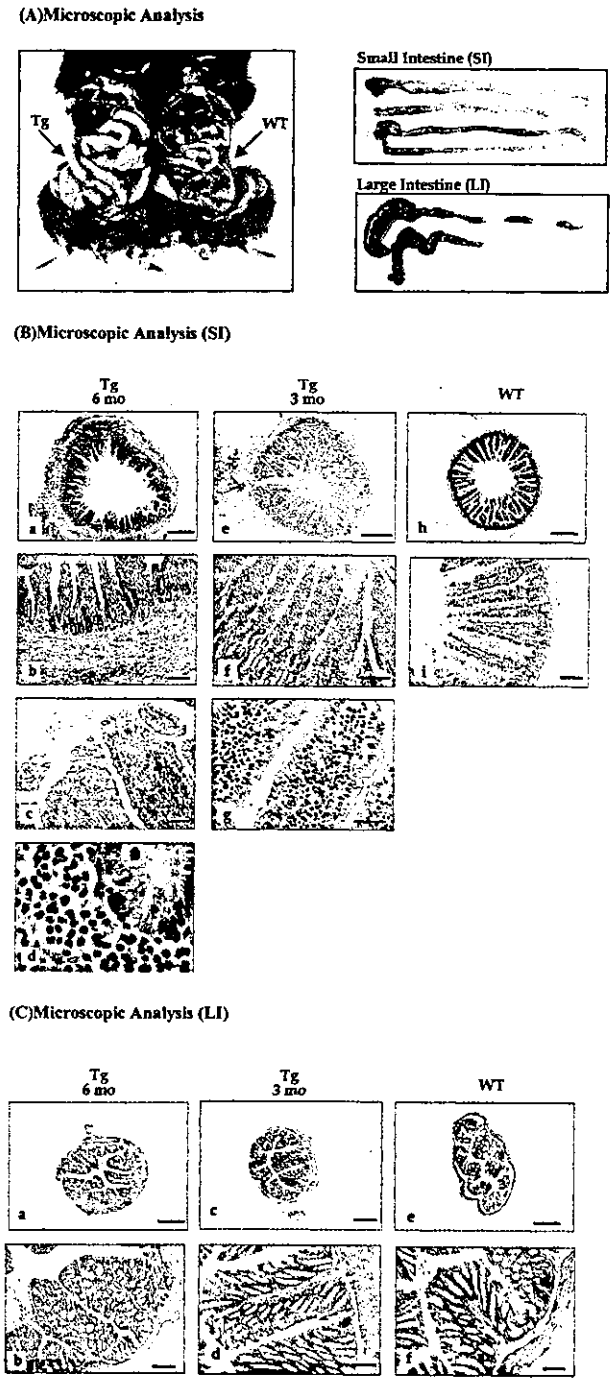

FIGURE 2. Development of small but not large intestinal inflammation in T3^b-IL-15 Tg mice. Macroscopic views and photomicrographs of SI and LI taken from T3^b-IL-15 Tg and WT mice at 4 mo of age. *A*, Macroscopic photographs of Tg and WT mouse intestine; arrows indicate the SI. *Right panels*, The macroscopic changes of SI and LI from Tg and WT mice, respectively. *B* and *C*, The microscopic appearance of the SI and LI at different ages. Histologic analysis was done on H&E stained tissue sections from Tg-SI of a mouse with severe disease at the age of 6 mo (*B*, *a–d*), Tg-SI of a mouse with mild disease at the age of 3 mo (*B*, *e–g*), WT-SI (*B*, *h* and *i*), Tg-LI of a mouse with severe disease at the age of 6 mo (*C*, *a* and *b*), and the Tg-LI of a mouse with mild disease at the age of 3 mo (*C*, *c* and *d*), WT-LI (*C*, *e* and *f*). Histopathologic changes were present in the SI but not the LI of Tg mice. Cross sections of SI of Tg mice showed reduced villus length (*Bb*), marked lymphocyte infiltration (*B*, *a* and *b*), and vacuolar degeneration of the villlus epithelium (*c*). Bars in *B*, *a*, *e*, and *h*, and *C*, *a*, *c*, and *e* indicate 500 μm. Bars in *B*, *b*, *f*, *g*, and *i*, and *C*, *b* and *d* indicate 100 μm. Bars in *B*, *c* and *g* indicate 50 μm. The bar in *Bd* indicates 25 μm.

Infiltrating cells in small intestinal inflammatory lesions consist of both CD8$\alpha\beta^+$ and CD8$\alpha\alpha^+$ T cells, but the increase in the former T cells corresponded to disease activity in the small intestinal LP

As shown in Fig. 3*A*, the numbers of CD8$^+$ T cells, i.e., CD8$\alpha\beta^+$ and CD8$\alpha\alpha^+$ T cells, in the small intestinal LP of T3^b-IL-15 Tg mice were significantly increased compared with the numbers in WT controls ($9.40 \pm 1.23 \times 10^7$ (T3^b-IL-15 Tg) vs $0.706 \pm 0.173 \times 10^7$ (WT)). Also, the degree of intestinal pathology was proportional to the abundance of CD8$\alpha\beta^+$ T cells in the diseased mucosa. As the disease activity became more severe with age, the proportion of CD8$\alpha\beta^+$ T cells profoundly increased, so that at 6 mo of age, the proportion of CD8$\alpha\beta^+$ T cells was >80% of small intestinal LP mononuclear cells (Fig. 3*A*). In contrast, CD8$\alpha\alpha^+$ T cells dominated when compared with CD8$\alpha\beta^+$ T cells among the fraction of CD8$^+$ T cells in T3^b-IL-15 Tg mice that had no disease or only mild intestinal pathology (at 2–3 mo; Fig. 3*A*).

Surface Ag analysis of activation and memory markers on CD8$^+$ T cells in the small intestinal LP initially revealed a standard phenotype of CD44^{high} and CD25$^-$ for intestinal T cells (Fig. 3*B*). In contrast, an early activation marker, CD69, was up-regulated in T3^b-IL-15 Tg mice when compared with WT controls (Fig. 3*B*). It was important to note that the IL-2Rβ chain, but not the IL-2Rα chain, was up-regulated in CD8$\alpha\beta^+$ T cells of T3^b-IL-15 Tg mice when compared with WT controls (Fig. 3*B*). In contrast, IL-2Rβ chain was not up-regulated in CD8$\alpha\alpha^+$ T cells of T3^b-IL-15 Tg mice when compared with WT controls (Fig. 3*B*)

The infiltrating cells in draining lymph nodes of the intestine consist mainly of memory-type CD8$\alpha\beta^+$ TCR$\alpha\beta^+$ T cells in the T3^b-IL-15 Tg mice

Because increased numbers of activated CD8$\alpha\beta^+$ T lymphocytes were selectively present in small intestinal LP of the Tg mice (Fig. 3), we next tried to elucidate the phenotype of the infiltrating cells in the MLN. CD8$\alpha\beta^+$ cells in the MLN of T3^b-IL-15 Tg mice which were greatly increased compared with the numbers in WT controls ($46.3 \pm 20.1 \times 10^7$ (T3^b-IL-15 Tg) vs $0.861 \pm 0.173 \times 10^7$ (WT)). Mononuclear cells isolated from the enlarged MLN consisted exclusively of CD8$\alpha\beta^+$ T cells (Fig. 4*A*). The usage of TCR by these CD8$\alpha\beta^+$ T cells was restricted to α and β heterodimers, and high expression of CD44 and Ly-6C Ags was noted (Fig. 4*A*). When these CD44^{high}CD8$^+$ T cells were stained for an early activation marker, CD25, no expression was detected (Fig. 4*A*). Up-regulation of CD122 (IL-2Rβ chain), but not CD25 (IL-2Rα), was observed in the CD8$\alpha\beta^+$ T cells of the MLN from T3^b-IL-15 Tg mice compared with those from WT controls (Fig. 4*A*). Thus, the pattern of cell surface markers suggests that these expanded CD44^{high}CD8$^+$ T cells were resting memory-type T cells.

CD8$\alpha\beta^+$ T cells in T3^b-IL-15 Tg mice coexpressed NK1.1 molecules

Because IL-15 is important in the development and propagation of NK and NK-T cells (30, 31), it was important to elucidate whether the expanded CD8$\alpha\beta^+$ T cells express the NK marker. In the MLN and small intestinal LP of the T3^b-IL-15 Tg mice, T cells expressing both NK1.1 and CD8$\alpha\beta$ were increased (Fig. 4*B*). Populations of CD8$\alpha\beta^+$ T cells expressing the NK marker were not detected in the WT controls (Fig. 4*B*). An increase of the classical CD4$^+$ NK-T cells and NK cells was not observed by flow cytometric analysis in the T3^b-IL-15 Tg mice (data not shown). Thus, the overexpression of IL-15 induced a unique subset of CD8$\alpha\beta^+$ NK-T cells rather than CD4$^+$ NK-T cells.

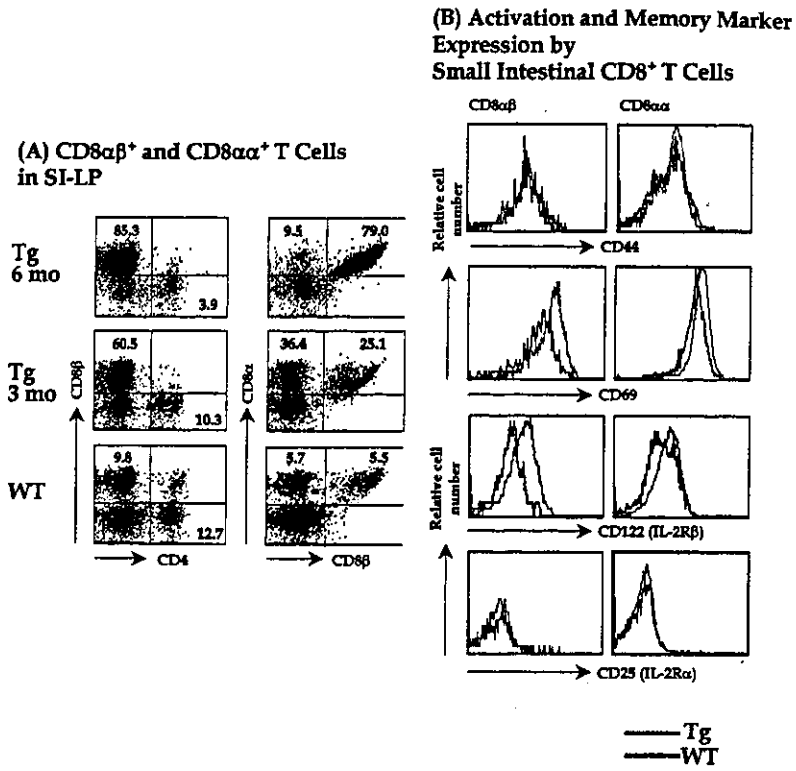

FIGURE 3. *A*, Flow cytometrical analysis of $CD8^+$ T lymphocytes isolated from small intestinal LP of $T3^b$-IL-15 Tg and WT mice. The percentage of total mononuclear cells is inserted in the gated boxes. *A*, The plots represent the most severe case at the age of 6 mo and the mild case at the age of 3 mo. The $CD8\alpha\beta^+$ and $CD8\alpha\alpha^+$ T cells in LP lymphocytes in $T3^b$-IL-15 Tg mice were significantly increased when compared with those in WT mice. *B*, The expressions of IL-2R subunits and activated/memory cell markers on $CD8\alpha\beta^+$ and $CD8\alpha\alpha^+$ T cells isolated from the small intestinal LP of $T3^b$-IL-15 Tg and WT mice were examined at the age of 6 mo. The expression of the β subunit of the IL-2 receptor and activated/memory markers were demonstrated on $CD8\alpha\beta^+$ and $CD8\alpha\alpha^+$ T cells. The results are representative of five independent experiments.

Dominant production of Th1-type cytokines by the increased $CD8\alpha\beta^+$ T cells in small intestinal LP of $T3^b$-IL-15 Tg mice

Cell-size analysis revealed that mononuclear cells isolated from the small intestinal LP of $T3^b$-IL-15 Tg mice had larger and more blastic features compared with cells from WT mice (Fig. 5*A*). Even though the expression of CD25 and CD44 by $CD8\alpha\beta^+$ T cells revealed a similar profile between the Tg and WT mice (Fig. 3*B*), the cell-sizing analysis suggested that a population of $CD8\alpha\beta^+$ T cells in the $T3^b$-IL-15 Tg mice possesses effector function rather than resting-memory function. This notion was further supported by the analysis of Th1- and Th2-type cytokine synthesis (Fig. 5*B*), where $CD8\alpha\beta^+$ T cells in the small intestinal LP of the Tg mice contained a significantly higher percentage of the Th1-type (IFN-γ and TNF-α) cytokine-producing cells than did those of WT mice. However, $CD8\alpha\alpha^+$ T cells, another increased population of $CD8^+$ T cells, did not produce Th1-type cytokines. There was no difference in IL-2 production by $CD8\alpha\beta^+$ and $CD8\alpha\alpha^+$ T cells between $T3^b$-IL-15 Tg and WT mice. In the diseased $T3^b$-IL-15 Tg mice, the degree of intestinal pathology paralleled the levels of production of Th1-type cytokines from the IL-15-induced $CD8\alpha\beta^+$ T cells in LP mononuclear cells (3 vs 6 mo; Fig. 5*B*). At 3 mo of age, $T3^b$-IL-15 Tg mice with mild pathology showed low levels of Th1-type cytokine production (Fig. 5*B*), but when the disease became more severe, at 6 mo of age, abundant Th1-type cytokines were produced by the IL-15-induced $CD8\alpha\beta^+$ T cells (Fig. 5*B*). In contrast, no synthesis of the Th2-type cytokines IL-4, IL-5, IL-6, and IL-10 was detected from $CD8^+$ T cells isolated from the small intestinal LP and MLN of $T3^b$-IL-15 Tg or WT mice (data not shown). $CD8\alpha\beta^+$ T cells in the MLN secreted low amounts of IFN-γ and TNF-α in comparison to the amounts secreted by small intestinal LP cells. Furthermore, to support this finding, the size of mononuclear cells isolated from MLN was smaller than that of intestinal LP cells (data not shown). The fact that increased levels of IFN-γ and TNF-α production by small intestinal $CD8\alpha\beta^+$ T cells paralleled the progression of inflammation suggests that these Th1-type cytokine-producing $CD8\alpha\beta^+NK1.1^+$ T cells are important in the development of intestinal inflammation.

Locally overexpressed IL-15 induced resistance to AICD in $CD8^+$ T cells from inflamed intestine of $T3^b$-IL-15 Tg mice

Because IL-15 has been shown to extend the survival of lymphocytes by inhibiting anti-Fas- or dexamethasone-mediated apoptosis (32), a possible explanation for the preferential expansion of $CD8\alpha\beta^+$ $NK1.1^+$ T cells in small intestinal LP and MLN could be the anti-apoptotic activity of IL-15. Therefore, we examined apoptotic activity of lymphocytes in inflammatory lesions of $T3^b$-IL-15 Tg mice by FACS analysis, using annexin V and propidium iodide. The overproduction of IL-15 in the SI caused a significant ($p < 0.05$) decrease in the percentage of annexin V-positive and propidium iodide-negative apoptotic LP cells in comparison to the situation in littermate controls (Fig. 6*A*). A similar finding was generated also by flow cytometric TUNEL analysis (Fig. 6*B*). These results suggest that locally overexpressed IL-15 induced resistance to AICD in $CD8\alpha\beta^+NK1.1^+$ T cells in the inflamed SI.

Discussion

Our primary aim in this study was to elucidate the role of mucosal IL-15 in the immunologic balance between intestinal immunity and inflammation. Thus, Tg mice carrying IL-15 cDNA under the control of $T3^b$-promoter were established to create an aberrant immunologic environment, with preferential overexpression of IL-15 in the intestinal tract. The fact that plural $T3^b$-IL-15 Tg lines developed mucosal inflammation indicates that this phenomenon was caused by itself and not by the positional effect of the transgene insertion into the chromosome. The artificial disruption of the tightly regulated expression of IL-15 in local sites should provide a useful experimental system for defining the role of IL-15 in mucosal pathogenesis. In contrast, the use of MHC class I promoter led to higher levels of IL-15 expression in the hematopoietic system (e.g., blood cells) and various organs (e.g., skin and lung; Ref.

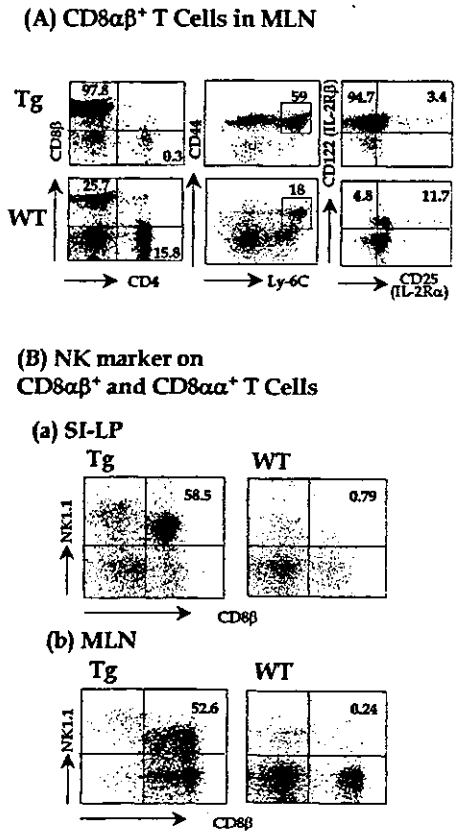

FIGURE 4. *A*, Flow cytometrical analysis of lymphocytes isolated from MLN of T3^b-IL-15 Tg and WT mice. Selective expansion of memory-type CD44^{high}, Ly-6C$^+$, CD8$\alpha\beta^+$ T cells in MLN was present in Tg mice. The percentage of specific marker positive cells is inserted in the gated boxes. The FACS profiles represent the most severe case at the age of 6 mo. The results are representative of eight independent experiments. *B*, The expression of NK1.1 Ag on CD8$\alpha\beta^+$ T cells isolated from small intestinal LP (SI-LP) and MLN of T3^b-IL-15 Tg with localized inflammation. Marked up-regulation of NK1.1 Ag was observed in T3^b-IL-15 Tg mice when compared with WT mice. The results are representative of eight independent experiments.

33) than in the T3^b-IL-15 Tg mice. The abundant expression in the hematopoietic system resulted in carcinogenic effects on lymphocytes leading to fatal leukemia. These two distinct IL-15 overexpression systems (e.g., local and systemic) provide a unique opportunity to understand the pathological effect of IL-15.

In the T3^b-IL-15 Tg mice, both CD8$\alpha\beta^+$ and CD8$\alpha\alpha^+$ T cells in the small intestinal LP were dramatically increased under the influence of overexpressed IL-15. Moreover, the increased numbers of CD8$\alpha\beta^+$ T cells, but not CD8$\alpha\alpha^+$ T cells corresponded to disease severity. This latter finding raised the possibility of a pathogenic role for CD8$\alpha\beta^+$ T cells in the intestinal inflammation of the T3^b-IL-15 Tg mice. Relevant to this possibility, an association of CD8$\alpha\beta^+$ T cells with autoimmune intestinal pathology has been reported (34, 35). A heat shock protein 60-specific CD8$^+$ T cell clone (34) or OVA-specific CD8$^+$ T cells (35) were associated with the development of intestinal inflammation on an autoimmune basis. Also, in inflammatory cutaneous lesions in IRF-2$^{-/-}$ mice, expansion of CD44^{high}, Ly-6C$^+$, and CD8$^+$ T cells was found responsible, and expression of IL-15 mRNA was increased in the skin (36). These reports support our finding that overexpression of IL-15 induced immunopathologic CD8$\alpha\beta^+$ T cells in experimental intestinal disease.

Although we observed an increase of CD8$\alpha\beta^+$ T cells in diseased T3^b-IL-15 Tg mice, we noted such an increase of CD8$\alpha\alpha^+$ T cells in mice that had no intestinal pathology as well. Because the number of CD8$\alpha\alpha^+$ T cells was decreased in the diseased mice, CD8$\alpha\alpha^+$ T cells could be a subset of regulatory T cells that can inhibit disease development. The increase of CD8$\alpha\alpha^+$ T cells is compatible with the reported appearance of CD8$\alpha\alpha^+$ T cells in the livers of IL-15 Tg mice that had no immunopathologic change despite having high levels of IL-15 expression (37). Furthermore, $\gamma\delta$ T cells, which constitute a major fraction of CD8$\alpha\alpha^+$ T cells, reportedly inhibited the development of airway hypersensitivity in the lung (38, 39). These findings, together with our observations in T3^b-IL-15 Tg mice, suggest that two distinct subsets of CD8$^+$ T cells, expressing $\alpha\beta$ or $\alpha\alpha$ dimers, exert opposing effects (pathologic vs inhibitory) in the intestinal inflammatory process. This interesting possibility is currently under intensive investigation in our laboratory.

IL-15 promotes the growth of IEL (11). However, in T3^b-IL-15 Tg mice we found no increase of any fraction of IEL despite the increased expression of IL-15 protein and mRNA. In contrast, there was an increase in the numbers of T lymphocytes isolated from the intestinal LP and MLN of the mice. IEC or IEC membranes can down-regulate the proliferative and cytokine responses of IEL (28). Thus, our results suggest that IEL and LPL CD8$^+$ T cells respond differently to the regulatory effects of IEC.

Several murine models of CD4$^+$ T cell-mediated colitis have been attributed to an exaggerated Th1-type response manifested by extensive production of IFN-γ and TNF-α (40–42); neutralization of IFN-γ and TNF-α with mAbs substantially improved intestinal inflammation in several of these models (40, 43). It has been reported also that the involvement of IFN-γ and TNF-α in small intestinal pathology by a heat shock protein 60-specific CD8$^+$ clone (34) supported the role of Th1-type cytokines produced by CD8$\alpha\beta^+$ T cells in the pathogenesis of inflammation. Together with the Th1-type cytokine profiles, our results in the cell-sizing analysis and CD69 expression of the IL-15-induced CD8$\alpha\beta^+$ T cells further indicate that the locally expanded intestinal CD8$\alpha\beta^+$ T cells have effector functions.

Recent studies have shown that CD8$^+$ T cells could acquire NK1.1 and NK cell-associated molecules in both in vitro and in vivo situations (44–46). IL-2, IL-4, and IL-15 can induce the expression of NK1.1 and NK cell-associated molecules on CD8$\alpha\beta^+$ T cells after in vitro culture under the dependent manner of cytokine signaling via IL-2Rβ chain. Furthermore, influenza viral infections and lymphocytic choriomeningitis virus induced virus-specific effector CD8$^+$ T cells expressing NK1.1 markers (45, 46). Our present findings directly demonstrated that overexpression of mucosal IL-15 created an immunologic environment favorable for the development of CD8$\alpha\beta^+$ T cells expressing NK1.1. Although the biological significance of NK1.1 expression by pathologic CD8$\alpha\beta^+$ T cells is unknown, the development and activation of CD8$\alpha\beta^+$NK1.1$^+$ T cells in response to the abrogation of the negative regulatory influence of IL-15 accompanied the development of small intestinal inflammation.

The intestinal inflammation in our T3^b-IL-15 Tg mice was not accompanied by an increased production of IL-2 or expression of IL-2Rα by CD8$\alpha\beta^+$NK1.1$^+$ T cells. This finding suggests that the Th1-type CD8$\alpha\beta^+$NK1.1$^+$ T cells were not driven by the growth and activation signals of IL-2. Furthermore, IL-2 and IL-15 seem to differently affect the survival and death of memory-type CD8$^+$ T cells under the condition of AICD (37, 47). IL-2 can promote AICD of T cells, while IL-15 inhibits the AICD pathway. The independence of CD8$\alpha\beta^+$ NK1.1 T cells from the effects of IL-2 may further promote the avoidance of AICD-associated apoptosis by pathogenic CD8$^+$ T cells. The balance between the expansion of autoreactive T cells and their rapid elimination by AICD is